Spacings and Neutron Widths of Nuclear Energy Levels*

J. A. HARVEY, D. J. HUGHES, R. S. CARTER, AND V. E. PILCHER
Brookhaven National Laboratory, Upton, New York
(Received February 28, 1955)

The parameters of nuclear energy levels at excitation energy just above neutron binding have been studied for about 20 heavy nuclides. Total cross sections for neutrons of energy 0 to 700 ev were made utilizing the Brookhaven fast chopper and the transmissions were analyzed to obtain the resonance parameters. The reduced neutron widths, Γ_n^0, show a wide variation among the resonances in single nuclides relative to radiation widths, Γ_γ. Within experimental error, the size distribution of the reduced neutron widths is exponential, the most probable width being zero. The experimental level spacings, D, exhibit discontinuities at closed shells, an effect that remains after correction of the spacings for differences in excitation energy. The ratio $\bar{\Gamma}_n^0/D$, of particular significance to the "cloudy crystal ball" nuclear model, has a maximum about $A=160$, as expected from theory, but of a much smaller magnitude than the computed peak.

I. INTRODUCTION

THE Brookhaven fast chopper has already been described as well as its initial use in measurement of parameters of neutron resonances in the neutron energy range 2–200 ev.[1] In these measurements the total cross section alone, obtained from sample transmission, was treated with no attempt to determine directly the partial cross sections, usually consisting of capture and scattering. The concentration on total cross sections was a result primarily of the nature of the fast chopper, in particular its small sample size and large detector area, which makes it particularly suitable for total cross section measurement by transmission.

Although the limitation to total cross section alone seems at first sight to neglect important parameters of levels, such as the partial widths Γ_n and Γ_γ, it has resulted that most of the level parameters can be obtained rapidly and with sufficient accuracy for comparison with theory by total cross section measurements alone. The analysis of the experimental data that makes possible the attainment of most of the level parameters is presented in Sec. II. It is indeed fortunate that so much information can be obtained from total cross sections because direct measurements of the partial cross sections, scattering[2] and capture,[3] are extremely difficult to perform and to interpret.

Because of these advantages, a vigorous program for measurement of total cross sections has been carried on for the past year, with the result that some 300 resonances have been studied during this period. The level parameters obtained represent a great increase in the available data for comparison with predictions of nuclear structure theory[4] relating to level widths and spacings. In addition, the measured parameters exhibit trends that have not been discussed theoretically, for example the "exponential Γ_n^0 distribution" presented in Sec. IV A; these results constitute the raw material for further theoretical development. In the present report the discussion will be devoted primarily to level spacings D, and neutron widths Γ_n, because of the relevance to nuclear models of current interest.[5,6] During the period under discussion a large number of radiation widths Γ_γ have also been measured; a summary of the earliest of these has already been published[7] and a more complete description will appear later.[8] In addition, a brief report[9] has been made on the ratio of neutron widths to level spacings, of special applicability to the "cloudy crystal ball" model.[5]

The information that was available in the past on level spacing obtained from neutron resonance data was very fragmentary and uncertain. In the present work it has been possible to measure enough resonances in a given energy interval in such a way that essentially all levels are located. In this way an unambiguous determination of the average level spacing[10] for the two possible spin states that can be formed by slow neutrons is made. The level spacings thus obtained are valuable for comparison with the predictions of various nuclear models because they are the spacings at neutron binding energy, hence about 7-Mev excitation, an energy at which the spacings were not well known previously. At the beginning of this work very little was known and nothing predicted by theory concerning the variation in neutron width from level to level, hence it was obviously desirable to measure individual Γ_n's for a number of levels.

* Work carried out under contract with U. S. Atomic Energy Commission.

1 Seidl, Hughes, Palevsky, Levin, Kato, and Sjöstrand, Phys. Rev. **95**, 476 (1954).
2 J. Tittman and C. Sheer, Phys. Rev. **83**, 746 (1951); H. L. Foote, Jr., Phys. Rev. **94**, 790 (1954); R. E. Wood, Phys. Rev. **95**, 644 (1954).
3 Albert, Yeater, and Gaerttner, Phys. Rev. **95**, 644 (1954); Gaerttner, Yeater, and Albert, Knolls Atomic Power Laboratory Report KAPL-1084, March, 1954 (unpublished); E. Meservey, Phys. Rev. **96**, 1006 (1954).
4 J. M. Blatt and V. F. Weisskopf, *Theoretical Nuclear Physics* (John Wiley and Sons, Inc., New York, 1952).
5 Feshbach, Porter, and Weisskopf, Phys. Rev. **96**, 448 (1954).
6 A. Bohr and B. R. Mottelson, Kgl. Danske Videnskab. Selskab, Mat.-fys. Medd **27**, 159 (1953).
7 D. J. Hughes and J. A. Harvey, Nature **173**, 942 (1954).
8 J. S. Levin (to be published).
9 Carter, Harvey, Hughes, and Pilcher, Phys. Rev. **96**, 113 (1954).
10 The symbol D is used through this paper to represent the level spacing for a single spin state.

Furthermore, the ratio of neutron width to level spacing was of obvious interest because predictions for this ratio did exist for the strongly absorbing or "black" nucleus and the partially transparent or "cloudy crystal ball" nuclear model. It is interesting that for both Γ_n and D large variations have been found, variations unexpected from current theory.

II. ANALYSIS OF DATA

The neutron resonance data are recorded in terms of sample transmission T, and the purpose of the analysis is to obtain all possible information about the level parameters from T as a function of neutron time-of-flight. Even though the transmission is a direct measure of the total cross section alone, the analysis gives much additional information concerning the parameters of the levels that appear as resonances in the total cross section. The partial cross sections for scattering and absorption that make up the total cross section (assuming no α or proton emission or fission) are given in terms of the level parameters by the Breit-Wigner single-level formula:

$$\sigma_s=4\pi\lambda\!\!\!^{-}{}_0^2 g\left|\frac{\Gamma_n/2}{E-E_0+i\Gamma/2}+\frac{R}{\lambda\!\!\!^{-}{}_0}\right|^2+4\pi(1-g)R^2, \quad (1)$$

and

$$\sigma_a=\pi\lambda\!\!\!^{-}{}_0^2 g\left(\frac{E_0}{E}\right)^{\frac{1}{2}}\frac{\Gamma_n\Gamma_\gamma}{(E-E_0)^2+(\Gamma/2)^2}, \quad (2)$$

where

$$g=\tfrac{1}{2}\left[1\pm\frac{1}{2I+1}\right]. \quad (3)$$

In these equations E is the energy of the neutron, $2\pi\lambda\!\!\!^{-}{}_0$ is the wavelength of a neutron with energy E_0, the energy at resonance, and Γ_n, Γ_γ, and Γ are the neutron, radiation, and total widths of the level. In practice the effect of levels other than that being analyzed, neglected in these equations, is often important but their effect can be subtracted by means described by Seidl *et al.*,[1] which will not be repeated here.

If the statistical factor g is known, the total cross section measurement alone gives the parameters of the level, Γ_γ and Γ_n (again assuming that other widths are negligible). This procedure is possible because the width of the cross section resonance at half-maximum is just Γ and the peak height σ_0 of the total cross section is given by

$$\sigma_0=4\pi\lambda\!\!\!^{-}{}_0^2 g\Gamma_n/\Gamma. \quad (4)$$

For a level at low neutron energy, where the instrumental resolution is very good, the procedure is relatively uncomplicated. In this region the *measured* peak height of the cross section resonance together with its width give Γ_γ and Γ_n (if g is known) after calculated corrections are made for the Doppler broadening of the level, as described by Seidl *et al.*[1]

If g is not known, as is usually the case, the method gives $g\Gamma_n$ rather than Γ_n. Measurement of the partial cross sections σ_s or σ_γ, which give Γ_n/Γ or Γ_γ/Γ, can be used to distinguish the correct choice of the two possible values of g in this case and thus all the parameters, including the spin of the compound state, J, are fixed. Use of the measurement of one of the partial cross sections (relative to the total) to fix g alone rather than to determine the other parameters is advisable because partial cross section measurements are inherently more complicated and difficult than transmission measurements.

As the partial cross-section measurements have been made for an exceedingly small number of resonances, the total cross-section work can be considered in general to give primarily Γ and $g\Gamma_n$ in the good resolution region. The important quantity Γ_γ can fortunately also be obtained rather well (from $\Gamma_\gamma=\Gamma-\Gamma_n$) because the uncertainty of g does not produce a large error in Γ_γ, as $g\Gamma_n$ is usually small compared to Γ.

For most of the measured Γ_γ's the experimental error is larger than the uncertainty arising from the two possible g values, even when this uncertainty is maximum, for $I=\frac{1}{2}$, in which case $g=\frac{1}{4}$ or $\frac{3}{4}$. A typical example of the $I=\frac{1}{2}$ case is the 17.6-ev level in thulium, described in III A, with a Γ of 63 ± 16 mv (millielectron volts) and a Γ_n of 1.5 or 4.5 mv depending on g. Here the uncertainty in Γ_γ arising from g (±1.5 mv) is less than the experimental uncertainty in Γ in spite of the fact that the two possible values of g have the maximum spread in this case. For other initial target spins the g uncertainty is less than it is for $I=\frac{1}{2}$, and there is no uncertainty for a zero-spin target nucleus, for which $g=1$. In contrast to Γ_γ values, the Γ_n's resulting from the measured $g\Gamma_n$'s contain an uncertainty that is a maximum of ±50 percent for $I=\frac{1}{2}$. However, the observed great range of measured Γ_n's implies that the uncertainty arising from g is not a serious handicap at the present stage of neutron spectroscopy.

Thus far we have considered only the case of good resolution, where results obtained with a single sample, usually thin, give all the needed information. For neutron energies somewhat higher than the good resolution region, however, the true shape of a resonance is greatly distorted by the resolution function and the analysis becomes extremely complicated. Nevertheless it is still possible, by measurement of both thin and thick samples, to obtain Γ and $g\Gamma_n$. The complication of the analysis is caused principally by the distorting effect of the Doppler broadening of the resonance and the change in the observed resonance shape with sample thickness. For the present work the method of analysis used in the poor resolution region is the same in principle as that described by Seidl *et al.*, but contains a few improvements. These improvements result in a great saving of time in the complicated analysis, which involves the areas of dips in transmission curves for two sample thicknesses and the Doppler broadening. This information is used to obtain σ_0 and Γ, the principle being illustrated by Fig. 1, and $g\Gamma_n$ and Γ_γ are then

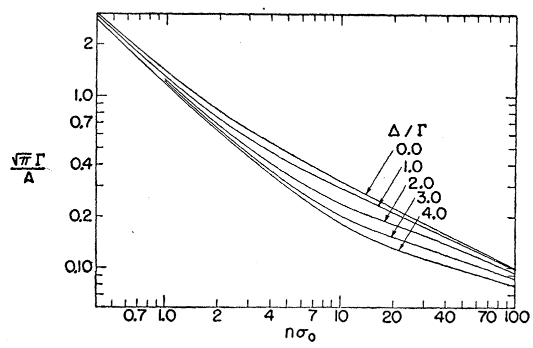

FIG. 1. Curves relating the measured area of transmission dips, A (ev), sample thickness n (atoms/cm^2), and Doppler broadening Δ (ev) to the resonance parameters Γ and σ_0 (peak height). The principle of the method of resonance analysis is that values of A, n, and Δ for two sample thicknesses are consistent with only a particular location on a single curve, and this location determines Γ and σ_0. (See reference 1.) Because the desired parameters appear combined with the measured quantities, the method involves successive approximations.

calculated as already described for the good resolution case.

It is fortunate that the results obtained are still valuable when, for experimental reasons, two sample thicknesses cannot be used. In general, at high energy only a thick sample can be used because a thin sample would give a transmission too close to unity for accurate results. However there are cases even at high energy in which, because of overlapping of resonances, only a thin-sample result is obtained. If a thin-sample result alone is available the quantity $\sigma_0\Gamma$ is obtained, which quantity gives $g\Gamma_n$ for the resonance directly with no knowledge of Γ necessary, as is seen from Eq. (4). For a thick-sample run alone, on the other hand, one obtains $\sigma_0\Gamma^2$, that is, $g\Gamma_n\Gamma$, and from this combination $g\Gamma_n$ is obtained only if Γ_γ is assumed. For cases in which a single thickness is available in the intermediate thickness range, a dependence of the resulting $g\Gamma_n$ on the assumed Γ_γ is present but weaker than for the thick sample. Because the main objective in the present work is the measurement of neutron widths, the dependence of $g\Gamma_n$ on the assumed Γ_γ was studied for each level in order to estimate the error of the final neutron widths.

The general procedure followed in determining $g\Gamma_n$ was to measure both it and Γ when two sample thicknesses could be used to give a reasonably accurate value of the latter. For resonances for which Γ could be measured only with large error or where just one sample thickness could be used, Γ_γ was taken to be the average of the measured values for other resonances in the same nuclide. The use of this "assumed" Γ_γ in getting Γ and hence $g\Gamma_n$ is fortunately not a source of great error because of the fact that the radiation widths are relatively constant compared to the extremely wide range that was found in this work for the Γ_n's. In addition, for many samples of intermediate thickness the error resulting from the Γ_γ "assumed" is much less than the experimental error because of the weak dependence of $g\Gamma_n$ on Γ_γ, as will be exemplified in the next section.

For most of the elements investigated, a sufficiently large number of resonances was found so that some statistical information was obtained on the distribution of level parameters among the levels of single nuclides. It was possible to investigate the distribution of level spacings in a given nuclide as a function of neutron energy and to use this observed distribution to determine at which energy a significant fraction of the levels was missed. The number of levels for some of the elements was sufficiently large so that the distribution law of the neutron widths, which would range over a factor as large as 100 for a given isotope, could be determined. Some general conclusions about this statistical information will be given in Sec. IV after the measurements of individual elements are described in Sec. III. In connection with the description of measurements, the manner in which average neutron widths, spacings, and width-to-spacing ratios are determined will be discussed.

III. MEASUREMENTS

The fast chopper, neutron detectors, and timing equipment have already been described in reference 1 and were used in essentially the same form during the past year with the exception of a few improvements. The chopper is a rapidly rotating shutter that produces neutrons in bursts of about 1-μsec duration, from which individual neutron velocities are selected electronically by the flight time to detectors 20 meters distant. The rotor is now being used regularly at a speed of 10 000 rpm compared to the 6000 rpm described in reference 1.

Previously the principal contribution to timing uncertainty was the time involved in pulse collection in the 2-in. diameter BF_3 neutron counters. A faster neutron counter has now been developed[11] and is in routine use. It consists of 128 counters, $\frac{3}{4}$ in. in diameter, in a common BF_3 atmosphere and operating at the same high voltage. The spread in pulse collection time for this multiple BF_3 counter is about 0.5 μsec (full width at half-maximum), and this time does not constitute a serious contribution to the final resolution function. As the neutron flight path in the multiple BF_3 counter is $3\frac{1}{2}$ in., the corresponding flight time becomes serious for neutrons below 20 ev for at this energy the flight time in the counter is 1.4 μsec. The flight time in the counter is much smaller in a scintillation-type detector that has been under development in the past year, but this detector is not in routine use as yet.

At high energies, where the flight time in the counter is negligible, the resolution function (with the multiple BF_3 counter) has a full width at half-maximum of 1.4 μsec, giving a resolution of 0.07 μsec/m at 20 meters. This resolution represents an energy spread of 2.0 ev at 100 ev and 22 ev at 500 ev. Under these conditions, the

[11] H. Palevsky (to be published).

TABLE I. Levels in thulium ($_{69}Tm^{169}$) with resonance energies (E_0) less than 160 ev. The neutron widths (Γ_n) are obtained from the measured areas of transmission dips for sample thicknesses n (atoms/cm²); r is the ratio of the error in Γ_n arising from the uncertainty in Γ_γ (taken as 70±20 mv for each resonance) to that arising from the area measurement. The statistical weight factor, g, is assumed to be $\frac{1}{2}$; Δ is the Doppler broadening of the level.

E_0 (ev)	Δ (ev)	$(1/n)\times10^{24}$ (cm²/atom)	Area (% error) (ev)	Γ_n (% error) (mv)	r	Weighted Γ_n (mv)	Reduced width Γ_n^0 (mv)
3.92±0.03	0.047	1390	0.84 (9)	12 (30)	1.3	12±4	6±2
14.4±0.1	0.095	1390	0.33 (7)	5.7 (16)	0.7	5.7±0.8	1.5±0.2
		90	1.17 (6)	5.7 (29)	2.0		
17.6±0.2	0.10	1390	0.21 (10)	3.4 (15)	0.3	3.2±0.4	0.76±0.10
		90	0.81 (5)	3.0 (25)	2.1		
29.1±0.3	0.14	90	0.22 (27)	0.37 (36)	<0.1	0.37±0.13	0.07±0.02
35.2±0.4	0.15	1390	0.33 (12)	11.6 (20)	0.2	13±2	2.2±0.4
		90	1.39 (7)	16 (28)	1.3		
38.1±0.5	0.16	90	0.27 (16)	0.61 (20)	0.15	0.61±0.12	0.10±0.02
45.6±0.6	0.17	1390	0.19 (22)	6.8 (27)	<0.1	6.4±1.3	0.9±0.2
		90	0.84 (9)	5.9 (29)	0.7		
51.6±0.7	0.18	1390	0.19 (25)	7.8 (30)	<0.1	7.7±1.6	1.1±0.2
		90	0.90 (9)	7.6 (29)	0.7		
59.8±0.8	0.20	1390	0.38 (19)	22 (27)	0.11	24±5	3.1±0.6
		690	0.71 (12)	30 (25)	0.3		
		90	1.11 (15)	14 (42)	0.4		
66.8±1.1	0.20	1390	0.85 (13)	80 (22)	0.25	100±15	12±2
		690	1.36 (9)	105 (17)	0.3		
		90	3.9 (10)	119 (18)	0.6		
84.4±1.5	0.23	690	0.36 (29)	14 (38)	<0.1	11±3	1.2±0.4
		90	0.87 (16)	9 (42)	0.2		
96±2	0.24	690	1.04 (14)	79 (26)	0.25	74±11	7.6±1.1
		90	2.3 (9)	71 (19)	0.7		
104±2	0.25	90	0.43 (40)	2.7 (54)	<0.1	2.7±1.4	0.26±0.14
118±2	0.27	690	0.69 (22)	46 (33)	<0.1	41±12	3.8±1.1
		90	1.38 (20)	32 (50)	0.2		
128±3	0.28	90	0.84 (25)	10 (48)	0.12	10±5	0.9±0.4
139±3	0.29	90	1.6 (23)	45 (60)	0.2	45±30	4±2
158±4	0.31	690	1.43 (15)	180 (35)	0.12	160±40	13±3
		90	2.9 (16)	130 (30)	0.2		

upper energy limit at which resonances can be resolved depends greatly on the element under study, for the level spacing differs greatly from element to element as we shall see in the next section.

In describing the results of the measurements, we shall first consider thulium because the procedure applied to all the elements is here well illustrated without the complication of separated isotopes. Tin will be described next because the additional analysis necessary for separated isotopes can be made clear. The results of the remaining elements and isotopes can then be described briefly because of the similarity of the methods involved.

A. Thulium

Two grams of thulium oxide of 99.9 percent purity[12] were available for the transmission measurements. These measurements were made from 3 to 200 ev with the old bank of BF_3 counters and hence with a resolution poorer than now available. Three sample thicknesses were used, $\frac{1}{2}$ in., $\frac{1}{16}$ in., and $\frac{1}{32}$ in., the thickest sample requiring only 0.75 g of sample in each of the two sample-holders because of the small cross-sectional area of the two neutron beams. The number of atoms/cm² for each of the samples is given in Table I. The error in the thickness of the thickest sample was about 4 percent and in the others about 6 percent. Runs were made sufficiently long to obtain about 2 percent statistical accuracy per point, one-μsec timing channels being used above 20 ev, two-μsec channels from 20–10 ev, and four-μsec channels below 10 ev. It was not necessary to make long runs for the open beam because its shape was well known from earlier runs. The procedure for determining the background was discussed in reference 1.

Transmission curves for thick and thin samples from 30–80 ev are shown in Fig. 2 on a time-of-flight scale. The resolution inferred from the observed widths at half-maximum of the small transmission dips was 3.4 μsec or 0.17 μsec/m. Between resonances the transmission of the thick sample is 0.86±0.02, which value gives 8±2 b for the potential scattering after correcting for the oxygen contribution. The areas of the transmission dips were measured with a planimeter on the curve of

[12] Obtained from Dr. F. H. Spedding, Ames Laboratory, Iowa, who also supplied the Tb, Ho, and Lu samples.

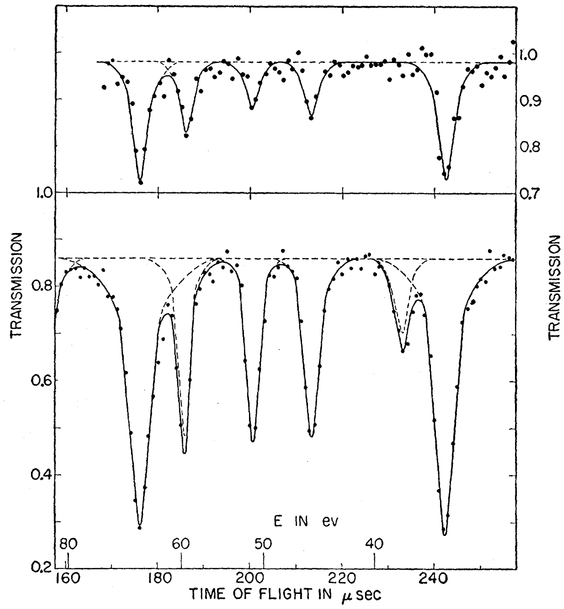

FIG. 2. The transmission as a function of time of flight at 20 m for thin ($1/n=1390$ cm²/atom, upper curve) and thick ($1/n=90$ cm²/atom, lower curve) samples of Tm_2O_3. The dotted straight line is the base line from which the areas of the resonances are measured. The analysis of these data by the method sketched in Fig. 1 is given in Table I.

Fig. 2, then normalized to unit transmission (i.e., divided by 0.86 for the resonances in the thick sample) and converted to ev. In the normalization, small corrections were made in the case of the 38.1- and 59.8-ev resonances because of the distorting effect of nearby large resonances. For each resonance, the area was measured over a limited energy interval, such that the wing correction (an area of $n\sigma_0\Gamma^2/\Delta E$, where ΔE is the energy interval) varied between 2 percent and 10 percent. The statistical errors quoted in Table I for the areas were calculated from the statistical accuracy of the points and the error in obtaining the "base line" used for normalization. The time-of-flight scale was accurate to ± 1 μsec.

For resonances where accurate data are available for both thick and thin samples, both Γ and σ_0 can be obtained since the thick and thin samples give approximately $\sigma_0\Gamma^2$ and $\sigma_0\Gamma$. In this case Γ_γ can be obtained even though the value of g ($\frac{1}{4}$ or $\frac{3}{4}$ for thulium) is not known, as discussed in Sec. II. For an intermediate sample, the power of Γ obtained is between 1 and 2. For example, the 35.2-ev resonance gave $\sigma_0\Gamma^{1.93}=59\pm10$ for the thick sample, and $\sigma_0\Gamma^{1.14}=310\pm50$ for the thin sample, by the technique illustrated in Fig. 1. From these numbers, Γ is obtained directly as 120 ± 40 mv and hence Γ_γ is 110 ± 40 mv, with negligible error arising from the assumption that $g=\frac{1}{2}$. For the 14.4- and 17.6-ev resonances the Γ's were calculated to be 75 ± 22 mv and 63 ± 16 mv, respectively, giving Γ_γ's of 69 ± 22 mv and 60 ± 16 mv, respectively. These three resonances thus give an average Γ_γ of 70 ± 12 mv for thulium.

Although thick and thin samples were measured for most of the other resonances in thulium the accuracy was not sufficient to give values of Γ_γ better than about 50 percent. Since radiation widths are known to be almost constant from resonance to resonance in a particular nuclide,[7] a radiation width of 70 ± 20 mv was used for all the thulium resonances to calculate $2g\Gamma_n$,[13] instead of Γ_γ's measured for particular resonances. Table I summarizes the results for thulium up to 160 ev, giving the pertinent experimental data used to obtain the neutron widths. The Doppler width Δ is calculated from the formula $\Delta=2(kTE_0m/M)^{\frac{1}{2}}$, with m/M the neutron-nucleus mass ratio, and kT expressed in ev. The error in $2g\Gamma_n$ is a result of the error in Γ_γ, taken as 70 ± 20 mv, and the error in A; the ratio of these contributions is given as r. For thin samples it can be seen that the error in $2g\Gamma_n$ arising from the uncertainty in Γ_γ is unimportant. For example, for an r even as large as 0.3, the Γ_γ uncertainty increases the error in $2g\Gamma_n$ above that resulting from the area error by only 5 percent. The reduced neutron width $2g\Gamma_n^0$ (reduced to 1 ev by division of $2g\Gamma_n$ by $E_0^{\frac{1}{2}}$) has the same error as the neutron width, since the energy of the resonance is measured quite accurately. The value of $\sigma_0\Gamma^2$ for the 3.92-ev resonance measured by Sailor *et al.*[14] together with a Γ_γ of 70 ± 20 mv give 14 ± 4 mv for $2g\Gamma_n$, which agrees with the present measurement.

In the energy range from 3–75 ev, 10 resonances were found compared to 6 in the range 75–150 ev. There are no resonances below 3 ev.[14] Above 75 ev it is quite apparent from the transmission curve that small levels may have been missed or that the transmission dips at the higher energies may not be single resonances. Below 75 ev any resonance larger than $\frac{1}{5}$ of the smallest observed would be sufficiently large for observation. Figure 3 illustrates the method of obtaining the level spacing D from the observed location of resonances in energy. The dropping away of the observed number of

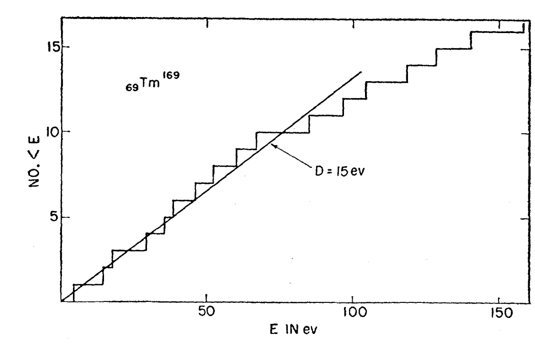

FIG. 3. The number of levels observed in thulium as a function of neutron energy. The slope of the straight line gives an observed spacing of 7.5 ev. On the assumption that the level spacing is the same for both spin states, D equals 15 ev for each spin state. It is apparent from the dropping away of the number of levels from the straight line that levels have been missed above 75 ev.

[13] Written thus because $2g$ is unity on the assumption that $g=\frac{1}{2}$.
[14] Sailor, Landon, and Foote, Phys. Rev. **96**, 1014 (1954).

levels below the straight line indicates that some levels are missed above 75 ev. The slope of the straight line corresponds to a level spacing of 7.5 ev for resonances of the two possible spin states, $J=I\pm\frac{1}{2}$. Assuming that there are the same number of levels of spin 0 and 1 (I for Tm is $\frac{1}{2}$) a value for D of 15 ev for each spin state is obtained.

The reduced neutron widths of the resonances vary over a wide range (greater than a factor of 100). The average value of $2g\Gamma_n^0$ for the first 10 resonances (up to 75 ev) is 2.8 ± 0.6 mv. In order to investigate the distribution of these ten reduced widths, the integral of the number of levels *versus* width is plotted in Fig. 4. It is seen that the integral distribution can be fitted by an exponential, implying that the differential distribution itself is exponential within experimental error. A complication in determining the distribution law arises because of the two possible values of g. For example, if the level spacings of the two spin states in thulium are the same, then (Sec. IV C) it is expected that the average reduced neutron widths, $\bar{\Gamma}_n^0$, of the two kinds of levels would be the same. The distribution of $2g\Gamma_n^0$ would then actually contain two groups, of equal numbers of resonances and equal $\bar{\Gamma}_n^0$ but differing by a factor of three in $2g\bar{\Gamma}_n^0$ ($g=\frac{1}{4}$ or $\frac{3}{4}$). The observed composite distribution would then depart from an exponential behavior simply because of lack of knowledge of g.

Although the level spacing and the distribution law of the reduced neutron widths are obtained from the first 10 resonances, 15 resonances can be used to obtain the $\bar{\Gamma}_n^0/D$ ratio, whose significance is discussed in Sec. IV C. The greater usable energy range for $\bar{\Gamma}_n^0/D$ results from the fact that this ratio (averaged over the two spin states) is simply the sum of $g\Gamma_n^0$ for all the resonances in a certain energy range divided by the range. Thus if small resonances are missed above 75 ev they have a very small effect on the sum, hence on $\bar{\Gamma}_n^0/D$. Also, for thin samples, if a transmission dip is really a combination of

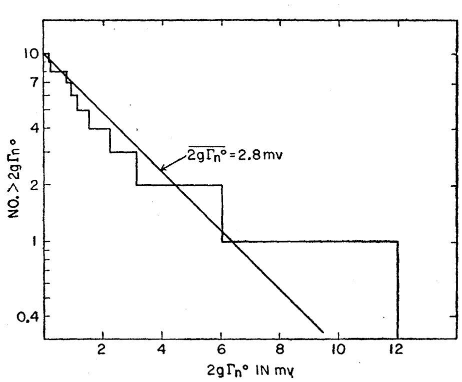

FIG. 4. The distribution of reduced neutron widths of the first 10 levels in thulium. The number of resonances with widths exceeding a particular value is plotted against this value. The straight line represents an exponential distribution with an average $2g\Gamma_n^0$ of 2.8 mv, which is the arithmetic average of the 10 widths. The slight curvature may be caused by the 2 spin states as discussed in the text.

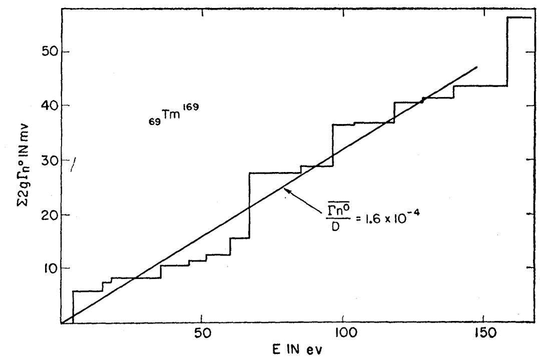

FIG. 5. The sum of the reduced neutron widths in thulium *vs* energy. A value of 1.6×10^{-4} for the $\bar{\Gamma}_n^0/D$ ratio is obtained from the straight line.

two unresolved resonances, the value of $g\Gamma_n^0$ computed in the analysis is just the sum of the two individual $g\Gamma_n^0$'s. Figure 5 is a plot of the sum of reduced neutron widths *vs* energy. The slope of the straight line gives directly the ratio $\bar{\Gamma}_n^0/D$. In the energy range up to 75 ev the stepped curve deviates from the straight line more than it does in the D plot of Fig. 3 since the Γ_n^0's show large fluctuations. On the other hand, the data in Fig. 5 above 75 ev do not drop away from the straight line as much as the D plot for the reasons just given. The slope of the line in Fig. 5 corresponds to a value for $\bar{\Gamma}_n^0/D$ of $(1.6\pm0.3)\times10^{-4}$.

B. Tin

The total cross section of tin was first measured from 10–500 ev, using a thick sample (25.3 g/cm^2) of metallic tin of 99.97 percent purity. The results showed many resonances above 35 ev. In order to identify the isotopes responsible for these resonances, samples (oxides) enriched in the isotopes[15] 112, 115, 116, 117, 118, 119, 120, and 122 were run from 35–500 ev, with no measurement being made on samples enriched in 114 and 124. These results will be discussed in three energy regions, below 92, 92–210, and above 210 ev.

Figure 6 shows the transmission of samples of normal tin and the enriched isotopes 117, 112, 116, and 119 in the energy range 92–210 ev. The normal and enriched 117 sample runs were made with the new BF_3 detector and $\frac{1}{2}$-μsec timing channels, hence with a resolution of 0.07 μsec/m, and the enriched 112, 116, and 119 samples with the old BF_3 counters with 1- and 2-μsec channels. Seven resonances were found in normal tin at 96.5, 112, 122, 125, 141, 149, and 197 ev. From the enriched isotope runs, the 122, 125, and 197-ev resonances were assigned to 117, the 96.5-ev resonance to 112, the 112 and 149-ev resonances to 116, and the 149-ev resonance to 119.

Thick samples of 118, 120, and 122 ($\sim$3 g/cm^2) showed no resonances in the energy region of Fig. 6.

[15] Enriched isotopes were obtained on loan from the Isotope Research and Production Division of the Oak Ridge National Laboratory, Oak Ridge, Tennessee.

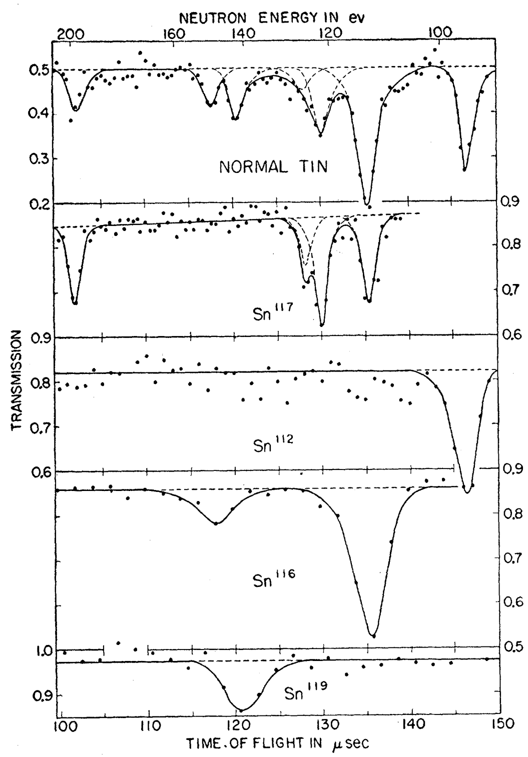

FIG. 6. The transmission as a function of neutron time of flight in the energy region 90 to 210 ev for samples of normal tin and enriched isotopes, illustrating the isotopic identification of resonances. The normal tin and 117 runs were made with a resolution of 0.07 μsec/m and the 112, 116, and 119 runs with a resolution of 0.2 μsec/m. The 112-ev resonance, actually in the 116 isotope, appears in the curve for the 117 sample because it contains appreciable 116. The fact that the base line is sloping in the 117 run is instrumental and does not introduce any error in the analysis of the resonances. The agreement between the parameters obtained from the normal run and the enriched isotope runs is obvious in Table II, where the experimental data and analysis are presented.

Although an enriched 124 sample was not run, the thick normal sample contained 1.58 g/cm^2 of 124 and any resonance in 124 would have been found. No 115 resonances were found in the 115 sample in the same energy range but this sample was enriched only to 14.0 percent in 115 (59.3 percent in 116) and only 0.5 g was available. It is possible that small resonances in 115 may have been missed, particularly near the large resonance in 116 at 112 ev. As the thick normal tin run contained 0.158 g/cm^2 of 114 and the 115 sample contained only 0.04 g/cm^2 of 114, it is possible that a small resonance may have been missed in 114. Thick- and thin-sample runs on the 112-ev resonance in 116 resulted in a Γ_γ of 110±40 mv.

There are three resonances in normal tin below 92 ev. No curve is shown for these resonances, which are at 39.4, 46.3, and 62.5 ev. From enriched isotope runs the 39.4-ev resonance is in 117 and the 46.3-ev resonance is in 118. The 62.5-ev resonance appeared in the 122 isotope run only, but the transmission dip was much too small to be assigned to 122. The 122 sample contained 3.07 percent 124, or 0.127 g/cm^2 of 124, and the observed dip for this sample thickness of 124 agrees with that calculated from the normal tin run on the assumption that the resonance is in 124. Thick and thin samples on the 39.4-ev resonance in 117 resulted in a Γ_γ of 106±25 mv. Any resonance larger than 1/100 of the observed resonances in the energy range below 92 ev would have been found.

In the energy range above 210 ev several of the observed transmission dips in the normal tin sample had contributions from more than one isotope. The transmission dip at 470 ev has contributions from 117 and 119, the dip at 425 ev has contributions from 117 and 120 and the 280-ev dip has contributions from 114 and 112. The fact that these dips have contributions from two isotopes is obvious from the enriched isotope runs. A large resonance in 118 at 268 ev also showed up in the enriched 117 sample, which contained 14.38 percent 118. The resonance at 222 ev was assigned to 119. Two small resonances at 260 and 340 ev which are barely seen in the normal tin run are reasonable resonances in the enriched 117 run. A resonance at 290 ev was found in the enriched 115 run but was too small to be seen in the normal tin run.

The pertinent data and the results of the analysis of the resonances are given in Table II in which a Γ_γ of 110±30 was used for each resonance. In addition to the columns explained for Table I, a column to indicate the sample (enriched isotope or normal) run is included. The agreement of the reduced neutron widths resulting from normal and enriched isotope runs is proof that the resonances have been correctly assigned to the various isotopes.

The level spacing and the $\bar{\Gamma}_n^0/D$ ratio for the Sn^{117} isotope was obtained by the same procedure described for thulium. There are five resonances below 300 ev in Sn^{117}, which give a D of 120±30 ev for each spin state, a $2g\bar{\Gamma}_n^0$ of 1.2±0.4 mv, and a value of $(0.10\pm0.04)\times10^{-4}$ for the $\bar{\Gamma}_n^0/D$ ratio. The results for the three higher resonances are not sufficiently accurate to include in the analysis. From the two resonances in 119 below 300 ev, a D of 300±140 ev is obtained. Since small resonances in 115 may have been missed, no value for D can be given for this isotope. For the even-even isotopes, only approximate values for D can be obtained because of the small number of levels found. Thus for the isotopes 112, 114, 116, 118, 120, 122, and 124, the spacings are 150±80, ~300, 150±70, 200±100, ~500, >500, ~200 ev, respectively. The observed spacing is the spacing for a single spin state as only the spin $\frac{1}{2}$ is possible for the compound nucleus. The $\bar{\Gamma}_n^0/D$ ratio averaged over all the even-even isotopes up to 300 ev can be obtained only with poor accuracy, giving $(0.20\pm0.08)\times10^{-4}$.

C. Other Elements

Molybdenum ($_{42}$Mo).—A thick sample (7.35 g/cm^2) of metallic molybdenum of 99.9 percent purity was run

TABLE II. Levels in tin isotopes ($E_0<500$ ev) based on measurements with normal tin and samples enriched in the various isotopes. The g factor is assumed to be $\frac{1}{2}$ for the odd, and unity for the even isotopes; Γ_γ is taken as 110 ± 30 mv; n refers to the particular isotope; other symbols have the same significance as in Table I.

Isotope	E_0 (ev)	Δ (ev)	Sample	$(1/n)\times10^{24}$ (cm²/atom)	Area (% error) (ev)	Γ_n (% error) (mv)	r	Weighted Γ_n (mv)	Reduced width Γ_n^0 (mv)
Sn^{112}	96.5 ± 2.0	0.29	112	880	1.53 (8)	95 (17)	0.5	85 ± 10	8.7 ± 1.0
			Normal	800	1.37 (10)	71 (19)	0.4		
	280 ± 9	0.51	112	880	0.5 (40)	36 (48)	<0.1	36 ± 17	2.2 ± 1.0
Sn^{114}	280 ± 9	0.50	Normal	1200	2.4 (20)	420 (23)	<0.1	450 ± 90	27 ± 5
			115	4600	1.3 (30)	540 (34)	<0.1		
Sn^{116}	112 ± 2	0.32	116	79	3.3 (15)	62 (25)	0.5	58 ± 6	5.5 ± 0.6
			Normal	55.2	3.6 (8)	55 (19)	0.9		
			Normal	1250	0.90 (10)	54 (16)	0.2		
			117	1990	0.75 (12)	62 (17)	0.2		
	149 ± 4	0.36	116	79	1.2 (30)	8 (70)	<0.1	4.5 ± 1.4	0.37 ± 0.11
			Normal	55.2	0.96 (20)	3.5 (34)	<0.1		
Sn^{118}	46.3 ± 0.6	0.20	118	44.9	0.71 (15)	0.7 (30)	0.3	0.7 ± 0.2	0.11 ± 0.03
			Normal	29.8	0.91 (18)	0.8 (50)	0.3		
	368 ± 14	0.57	118	40.7	10.7 (6)	410 (7)	0.4	420 ± 30	22.0 ± 1.3
			Normal	33.2	11.5 (9)	390 (11)	0.3		
			117	382	4.8 (12)	560 (17)	0.2		
Sn^{120}	425 ± 18	0.61	120	71	3.9 (25)	44 (40)	0.3	44 ± 18	2.1 ± 0.8
Sn^{122}	No resonances								
Sn^{124}	62.5 ± 0.9	0.23	Normal	130	1.35 (20)	11 (49)	0.4	12 ± 2	1.5 ± 0.3
			122	1620	0.22 (20)	12 (23)	<0.1		
Sn^{115}	290 ± 10	0.50	115	670	1.6 (30)	260 (50)	<0.1	260 ± 130	3.0 ± 1.5
Sn^{117}	39.4 ± 0.5	0.19	117	71	1.07 (6)	5.3 (24)	1.3	5.4 ± 0.5	0.86 ± 0.09
			117	1550	0.164 (10)	5.6 (11)	<0.1		
			Normal	94	0.87 (12)	4.3 (34)	0.4		
	122 ± 3	0.33	117	91	1.09 (12)	13 (23)	0.3	15 ± 3	1.4 ± 0.3
			Normal	104	1.43 (20)	27 (52)	0.2		
	125 ± 3	0.33	117	91	0.37 (30)	2.5 (36)	<0.1	2.8 ± 0.8	0.25 ± 0.08
			Normal	104	0.47 (50)	3.9 (65)	<0.1		
	197 ± 6	0.42	117	91	1.48 (15)	30 (29)	0.2	35 ± 9	2.5 ± 0.6
			Normal	104	1.7 (25)	52 (61)	0.15		
	259 ± 8	0.48	117	71	0.87 (25)	12 (36)	<0.1	12 ± 4	0.8 ± 0.3
	343 ± 13	0.55	117	71	2.2 (30)	80 (80)	<0.1	80 ± 60	4 ± 3
	425 ± 18	0.61	117	71	3.3 (22)	190 (40)	0.15	190 ± 80	9 ± 4
	460 ± 20	0.64	117	71	2.4 (25)	120 (60)	0.1	120 ± 70	6 ± 4
Sn^{119}	141 ± 3	0.35	119	138	1.6 (20)	52 (57)	0.2	30 ± 12	2.5 ± 1.0
			Normal	92	1.2 (20)	17 (48)	0.15		
	222 ± 7	0.44	119	138	0.98 (22)	24 (33)	0.15	24 ± 6	1.6 ± 0.4
			Normal	92	1.25 (18)	24 (33)	0.1		
	460 ± 20	0.63	119	138	2.6 (25)	200 (37)	0.1	200 ± 70	9 ± 3

from 10 to 750 ev with a resolution of 0.07 μsec/m. Twelve resonances were found and at the higher energies smaller resonances may have been missed. Samples of MoO_3 enriched in 95, 96, and 97 obtained from Oak Ridge were run over the same range. The other isotopes were not available in sufficient quantity to make suitable identification of resonances at the higher energies. The procedure for identifying the resonances is similar to that used for tin.

The data are summarized in Table III, based on a radiation width of 260 ± 80 mv. For the 45-ev and 71.5-ev resonances, measurements for various sample thicknesses gave values for Γ_γ. The measurements on the 45-ev resonance give $\Gamma=392\pm50$ mv, $2g\Gamma_n=186\pm20$ mv, and hence $\Gamma_\gamma=206\pm60$ mv. The 71.5-ev resonance has $\Gamma=344\pm80$ mv, $2g\Gamma_n=16\pm2$ mv, and $\Gamma_\gamma=330\pm80$ mv. Concerning isotopic assignments, the 45, 71.5, 133, 367, and 478-ev resonances are in the isotopes 95, 97, 96, 100, and 98, respectively.[16] Two apparently single resonances in the normal sample have contributions from more than one isotope. The 570-ev resonance has contributions from Mo^{95} and Mo^{97} and the 406-ev resonance has contributions from Mo^{97} and another isotope. The three resonances at 406, 440, and 510 ev could not be assigned to a definite isotope. The calcula-

[16] The three lowest-energy resonances have been identified previously by S. P. Harris, Argonne National Laboratory Progress Report ANL-5031, February, 1953 (unpublished).

TABLE III. Neutron widths of resonances in the isotopes of molybdenum ($_{42}$Mo) based on a Γ_γ of 260±80 mv.

Isotope	E_0 (ev)	Δ (ev)	Sample	$(1/n)\times10^{24}$ (cm²/atom)	Area (% error) (ev)	Γ_n (% error) (mv)	r	Weighted Γ_n (mv)	Reduced width Γ_n^0 (mv)
Mo^{95}	45.0±0.6	0.22	Normal	18 490	0.39 (6)	177 (8)	0.4	174±10	26.0±1.6
			Normal	7830	0.83 (12)	184 (15)	0.3		
			Normal	1890	1.82 (5)	163 (14)	1.7		
			Normal	409	3.96 (4)	161 (11)	2.0		
			Normal	137	7.2 (10)	177 (17)	1.0		
	162±4	0.42	95	83	1.14 (10)	11.6 (19)	0.6	13.6±1.9	1.1±0.2
			Normal	137	1.00 (12)	15.6 (20)	0.5		
	570±30	0.79	95	83	2.6 (30)	120 (50)	0.1	120±60	5±3
	700±40	0.87	95	83	7.5 (20)	740 (18)	0.2	740±130	28±5
Mo^{96}	133±2	0.38	96	1890	1.90 (6)	215 (13)	0.8	200±15	17.3±1.3
			96	62.7	8.1 (8)	160 (22)	1.1		
			Normal	17 600	0.38 (20)	240 (21)	<0.1		
			Normal	295	4.07 (7)	170 (21)	1.2		
			Normal	131	6.7 (6)	200 (21)	1.2		
			95	1340	2.02 (12)	180 (23)	0.6		
Mo^{97}	71.5±1.2	0.28	97	122	1.67 (5)	17.8 (27)	2.2	16.6±1.8	2.0±0.2
			Normal	1010	0.42 (15)	17.2 (19)	0.2		
			Normal	690	0.57 (16)	17.6 (21)	0.2		
			Normal	520	0.60 (15)	14.2 (21)	0.3		
			Normal	232	1.19 (22)	17.3 (43)	0.4		
	292±10	0.56	97	122	2.4 (15)	94 (32)	0.4	75±15	4.4±0.9
			Normal	232	1.33 (15)	63 (24)	0.3		
	406±17	0.66	97	122	1.9 (35)	80 (55)	0.1	80±40	4±2
	580±30	0.79	97	122	6.3 (25)	670 (20)	0.2	670±130	28±6
Mo^{98}	480±20	0.71	Normal	93	10.5 (12)	640 (21)	0.3	740±110	34±5
			95	2060	3.0 (25)	1000 (36)	<0.1		
			96	1640	3.0 (25)	860 (36)	<0.1		
			97	815	3.3 (25)	570 (39)	<0.1		
Mo^{100}	367±15	0.62	Normal	238	10.5 (10)	960 (18)	0.4	1000±120	52±6
			95	1130	5.1 (12)	1050 (19)	0.2		
			96	5380	1.6 (30)	900 (35)	<0.1		
			97	8360	1.3 (40)	1100 (46)	<0.1		
$Mo^{92,94,98,100}$	406±17	0.66	Normal	148[a]	1.4 (40)	30 (60)	0.1	30±18	1.5±0.9
	440±20	0.69	Normal	148[a]	2.9 (20)	110 (40)	0.3	110±40	5±2
	510±20	0.74	Normal	148[a]	2.7 (30)	110 (56)	0.2	110±60	5±3

[a] Average for the isotopes 92, 94, 98 and 100 as explained in text.

tions for these three resonances in Table III were based on an isotopic abundance of 14.6 percent (the average of the isotopes 92, 94, 98, and 100). The transmission between resonances gives a value of 5.4±0.3 b for the potential scattering cross section of molybdenum.

In the entire energy range investigated, four resonances were found in Mo^{95} and the same number in Mo^{97}. The level spacing D thus equals 370±120 ev for each isotope. The $\bar{\Gamma}_n^0/D$ ratios for Mo^{95} and Mo^{97}, based on these four resonances, are $(0.40\pm0.14)\times10^{-4}$ and $(0.26\pm0.09)\times10^{-4}$, respectively. There are six resonances up to 600 ev assigned to the five even isotopes, which results in an average level spacing for the five isotopes of 500±150 ev. The average $\bar{\Gamma}_n^0/D$ for these five isotopes is $(0.38\pm0.11)\times10^{-4}$.

Indium ($_{49}$In).—The transmissions of three samples of indium metal of thicknesses 9.14, 1.10, and 0.87 g/cm² were measured from 3 to 150 ev, and a 0.102 g/cm² sample from 3 to 10 ev, with a resolution of 0.17 μsec/m. A sample of In_2O_3 enriched to 60 percent In^{113} was run from 3 to 150 ev and one enriched to 99.94 percent In^{115} (2.32 g/cm²) from 43 to 150 ev, with a resolution of 0.07 μsec/m. The resonances and their assignments up to 40 ev agree with previous work with the Brookhaven crystal spectrometer[17] and the Oak Ridge fast chopper.[18]

Thick- and thin-sample runs on the 9.1-, 12.1-, and 40-ev resonances in In^{115} result in Γ_γ's of 80±40, 140±60, and 140±50 mv, respectively. Recent work with the Brookhaven crystal spectrometer[19] gives values of Γ_γ of 81±4 mv for the 3.86-ev resonance and 72±2 mv for the 1.46-ev resonance (both in In^{115}). In computing the neutron widths for In^{115} in Table IV, an average value of 77±15 mv was used. Thick- and thin-sample runs on the 14.7- and 25.2-ev resonances in In^{113} result in Γ_γ's of 60±20 and 110±40 mv, respectively. For all resonances in In^{113} in Table IV, an average Γ_γ of 80±20 mv was used.

[17] V. L. Sailor and L. B. Borst, Phys. Rev. **87**, 161 (1952).
[18] G. S. Pawlicki and E. C. Smith, Oak Ridge National Laboratory Quarterly Progress Report ORNL-1289, March 1952 (unpublished).
[19] H. H. Landon and V. L. Sailor (private communication).

TABLE IV. Neutron widths of resonances in the isotopes of indium ($_{49}In$) based on a Γ_γ of 80±20 mv for In^{113} and 77±15 mv for In^{115}.

Isotope	E_0 (ev)	Δ (ev)	Sample	$(1/n)\times10^{24}$ (cm²/atom)	Area (% error) (ev)	Γ_n (% error) (mv)	r	Weighted Γ_n (mv)	Reduced width Γ_n^0 (mv)
In^{113}	4.71±0.04	0.065	113	196	0.173 (11)	0.104 (15)	0.4	0.104±0.016	0.048±0.007
	14.7±0.1	0.12	113	196	0.93 (6)	6.1 (27)	1.5	7.7±1.0	2.0±0.3
			Normal	498	0.72 (8)	8.1 (25)	1.1		
			Normal	5250	0.20 (15)	8.2 (19)	0.2		
	21.7±0.2	0.14	113	196	0.71 (11)	4.2 (30)	0.8	4.4±0.9	0.95±0.20
			Normal	498	0.42 (20)	3.8 (36)	0.3		
			Normal	5250	0.081 (27)	5.0 (30)	<0.1		
	25.2±0.2	0.15	113	196	0.99 (10)	10.2 (30)	0.8	9.7±1.6	1.9±0.3
			Normal	498	0.67 (10)	10.0 (25)	0.7		
			Normal	5250	0.123 (22)	9.1 (23)	<0.1		
	32.5±0.4	0.17	113	196	0.80 (6)	7.3 (23)	1.1	8.5±1.0	1.49±0.18
			Normal	498	0.55 (12)	8.0 (24)	0.4		
			Normal	5250	0.13 (25)	12.5 (28)	<0.1		
	45.6±0.6	0.20	113	196	0.59 (12)	4.7 (26)	0.4	4.7±1.2	0.69±0.18
	63.6±1.0	0.24	113	196	0.15 (40)	1.0 (44)	<0.1	1.0±0.4	0.13±0.06
	70.6±1.2	0.25	113	196	0.48 (9)	4.7 (15)	0.3	4.7±0.7	0.56±0.08
	82.5±1.5	0.27	113	196	0.30 (30)	2.9 (36)	<0.1	2.9±1.0	0.32±0.11
	93.2±1.8	0.29	113	196	1.34 (9)	40 (20)	0.5	40±8	4.1±0.8
	105±2	0.31	113	196	1.15 (14)	29 (30)	0.3	29±9	2.8±0.9
In^{115}	3.86±0.04	0.059	Normal	1950	0.075 (10)	0.31 (11)	0.2	0.34±0.03	0.173±0.014
			Normal	230	0.408 (5)	0.43 (17)	1.4		
			113	294	0.316 (7)	0.33 (17)	0.9		
	9.10±0.09	0.090	Normal	1950	0.163 (10)	1.78 (12)	0.3	1.73±0.17	0.57±0.06
			Normal	230	0.55 (7)	1.6 (20)	1.0		
			113	294	0.51 (10)	1.7 (25)	0.7		
	12.1±0.1	0.10	Normal	21.8	0.46 (8)	0.131 (20)	0.9	0.106±0.013	0.031±0.004
			Normal	230	0.076 (20)	0.115 (23)	<0.1		
			113	294	0.047 (17)	0.088 (16)	<0.1		
	23.0±0.2	0.14	Normal	21.8	0.71 (10)	0.5 (30)	0.6	1.0±0.2	0.21±0.04
			Normal	230	0.34 (15)	1.3 (21)	0.2		
	39.9±0.5	0.19	Normal	21.8	1.47 (12)	4.6 (31)	0.8	3.5±0.4	0.55±0.06
			Normal	182	0.48 (15)	2.8 (26)	0.2		
			113	294	0.41 (8)	3.5 (12)	0.3		
	46.3±0.6	0.20	115	82.4	0.20 (17)	0.43 (21)	<0.1	0.43±0.09	0.063±0.013
	48.6±0.7	0.21	Normal	21.8	0.60 (12)	0.59 (23)	0.3	0.65±0.08	0.093±0.012
			115	82.4	0.28 (13)	0.69 (17)	<0.1		
	63.2±1.0	0.24	115	82.4	0.34 (21)	1.1 (28)	<0.1	1.1±0.3	0.14±0.04
	83.3±1.5	0.27	Normal	21.8	1.98 (10)	15 (30)	0.5	11±2	1.2±0.2
			Normal	182	0.60 (25)	7 (41)	<0.1		
			115	82.4	1.07 (12)	11 (32)	0.3		
	95±2	0.29	115	82.4	0.51 (14)	2.8 (21)	<0.1	2.8±0.6	0.29±0.06

In In^{113} there are seven resonances (including the 1.80-ev resonance measured by Sailor and Borst)[17] up to an energy of 49 ev, resulting in a D of 14±2 ev. Above this energy small resonances may have been missed or the ones given in Table IV may not be single resonances. The $\bar{\Gamma}_n^0/D$ ratio for In^{113}, obtained from a plot like Fig. 5 for Tm, is $(0.60\pm0.11)\times10^{-4}$. In In^{115} there are eight resonances (including the 1.46-ev resonance)[17] up to 56 ev resulting in a D of 14±2 ev. The $\bar{\Gamma}_n^0/D$ ratio for In^{115} (including a value of 2.78 mv for the Γ_n^0 of the 1.46-ev resonance)[19] is $(0.31\pm0.06)\times10^{-4}$. The reduced neutron width of the 1.46-ev resonance is unusually great, being about six times the average reduced neutron width.

Cesium ($_{55}Cs^{133}$).—The transmission of a thick sample of $CsNO_3$ (99.9 percent purity) was measured from 10 to 600 ev with a resolution of 0.07 μsec/m. A thin sample was run only below 60 ev. Thick- and thin-sample measurements on the 22.6- and 47.8-ev resonances gave Γ_γ's of 120±40 and 140±60 mv. The 5.9-ev resonance has been reported to have a Γ_γ of 115±20 mv and a $2g\Gamma_n$ of 5.2±0.4 mv.[20] An average Γ_γ of 110±30 mv was used for all resonances in the computations of Table V. There are 12 resonances up to 250 ev resulting in a D of 42±5 ev. The $\bar{\Gamma}_n^0/D$-ratio (including a value of 2.1 mv for the Γ_n^0 of the 5.9-ev resonance)[20] is $(1.0\pm0.2)\times10^{-4}$. The large resonance at 240 ev has a reduced neutron width about seven times the average reduced

[20] H. H. Landon and V. L. Sailor, Phys. Rev. **93**, 1030 (1954).

TABLE V. Neutron widths of resonances in cesium ($_{55}Cs^{133}$) based on a Γ_γ of 110±30 mv.

E_0 (ev)	Δ (ev)	$(1/n)\times10^{24}$ (cm²/atom)	Area (% error) (ev)	Γ_n (% error) (mv)	r	Weighted Γ_n (mv)	Reduced width Γ_n^0 (mv)
22.6±0.3	0.13	910 75.2	0.42 (12) 1.44 (7)	6.5 (21) 6.7 (27)	0.6 1.8	6.6±1.1	1.4±0.2
47.8±0.6	0.19	910 75.2	0.55 (12) 1.88 (10)	19 (19) 20 (28)	0.5 1.4	19±3	2.8±0.4
83.1±1.5	0.26	72.6	1.12 (13)	9 (33)	0.6	9±3	1.0±0.3
94.8±1.8	0.27	73.7	1.45 (10)	19 (29)	0.7	19±6	2.0±0.6
128±2	0.32	73.7	3.40 (7)	112 (17)	0.8	112±19	9.9±1.7
143±3	0.33	73.7	0.92 (25)	9 (45)	0.2	9±4	0.8±0.4
149±4	0.34	73.7	1.9 (20)	45 (43)	0.3	45±20	3.7±1.6
182±5	0.38	73.7	0.42 (25)	3.4 (30)	<0.1	3.4±1.1	0.25±0.08
204±6	0.40	73.7	2.0 (15)	57 (38)	0.4	57±22	4.0±1.5
224±6	0.42	73.7	1.8 (20)	49 (46)	0.2	49±22	3.3±1.5
240±7	0.44	73.7	8.1 (8)	480 (18)	0.3	480±90	31±6
301±10	0.49	73.7	3.5 (10)	190 (24)	0.4	190±40	11±2
370±14	0.54	73.7	3.0 (15)	160 (34)	0.2	160±60	8±3
407±16	0.56	73.7	7.3 (20)	570 (38)	0.1	570±200	28±11
443±19	0.59	73.7	4.2 (25)	290 (49)	0.1	290±140	14±6
530±25	0.64	73.7	9.0 (20)	800 (38)	<0.1	800±300	35±13

neutron width. The size distribution of the reduced neutron widths is shown in Fig. 7, in comparison with distributions for several other nuclides.

Europium ($_{63}$Eu).—Four thicknesses of europium oxide from 0.066 to 1.57 g/cm² of europium were run from 4 to 50 ev with a resolution 0.17 μsec/m. The europium oxide (reported to be 99.8 percent purity) was obtained from the Fordomes Trading Company. No analyses were made on the transmission of the thick samples at the higher energies since the resonances were not well resolved. Since Eu^{151} and Eu^{153} are nearly equally abundant, an average abundance of 50 percent was used to calculate the isotopic sample thickness. An average Γ_γ of 90±20 mv was used for all resonances in Table VI, this value being obtained from the average Γ_γ for the first three resonances.[21] Several of the small resonances listed in Table VI had not been observed in earlier work,[21] whereas the reported resonances at 6.3 and 7.4 ev have each been resolved into two resonances. A resonance was observed at 8.1 ev and is believed to be due to a Sm impurity since no resonance was found at this energy by Sailor, *et al.*[21] The area of the transmission dip corresponds to 1.7 percent Sm impurity. Although this is more than the reported purity of the sample would allow, we have omitted this resonance from Table VI. The other Sm resonances are not large enough to be observed in the Eu sample. It is possible that the 5.47-ev resonance is caused by a Dy impurity, for there is a strong Dy resonance at this energy.

If we include the eight resonances below 4 ev measured with the Brookhaven crystal spectrometer,[21] there are 14 resonances below 7.7 ev. Assuming the level spacing of each isotope and each spin state is the same, we obtain an average D of 2.2 ev for each spin state. Even though all resonances were not found above 8 ev, the ratio $\bar{\Gamma}_n^0/D$ obtained, as in Fig. 5 for Tm, utilizes all the data up to 30 ev since the samples were sufficiently thin. The ratio $\bar{\Gamma}_n^0/D$ thus obtained is $(2.3\pm0.3)\times10^{-4}$. The Γ_n^0 distribution is given in Fig. 7.

Terbium ($_{65}Tb^{159}$).—Two hundred milligrams of Tb_4O_7 of ~99 percent purity were obtained from Dr. F. H. Spedding. Three sample thicknesses (1.05, 0.53, and 0.205 g/cm²) were run from 3 to 200 ev with a resolution of 0.17 μsec/m. The data and the results are summarized in Table VII based on a Γ_γ of 90±30 mv. The Brookhaven crystal spectrometer group have recently studied the first three levels.[14] However, they also reported a resonance at 10.6±0.3 ev which we do not observe even though the thick sample run was sufficiently thick to see a good sized transmission dip if the resonance were as large as reported. There are 16 resonances up to 80 ev, whose size distribution is given in Fig. 7. The D is 10.0±1.0 ev, and the ratio Γ_n^0/D is $(1.5\pm0.2)\times10^{-4}$.

Holmium ($_{67}Ho^{165}$).—Thick and thin samples of holmium oxide (99.9 percent purity) were run from 3 to 200 ev with a resolution 0.17 μsec/m. In the thick sample run a small resonance was observed at 8.1 ev and is believed to be due to a Sm impurity. The data and the results are given in Table VIII based on a Γ_γ of 90±20 mv. This Γ_γ was obtained from the average value of the Γ_γ measured for six resonances. The measured values of Γ_γ for the 18.2, 35.9, 40.3, 48.5, 73.1, and 87.2-ev

[21] Sailor, Foote, and Landon, Phys. Rev. **93**, 1292 (1954) and private communication from H. H. Landon.

resonances were 180±90, 60±20, 60±30, 60±30, 140±70, and 260±130 mv.

In previous work on holmium,[14] the first four levels were measured. From the reported $\sigma_0\Gamma^2$ of 77 ± 10^{11} for the 3.9-ev resonance and a Γ_γ of 90±20, a value for $2g\Gamma_n^0$ of 2.5±0.7 can be obtained, which agrees with the value of 2.5±0.5 in Table VIII. The size distribution of the neutron widths of the 15 resonances up to 90 ev are given in Fig. 7. These levels give a D of 12.0±1.3 ev. The ratio of $\bar{\Gamma}_n^0/D$ is $(2.5\pm0.4)\times10^{-4}$.

Lutetium ($_{71}$Lu).—The transmissions of thick and thin samples of Lu_2O_3 (99.9 percent purity) were measured from 4 to 150 ev. Thick and thin runs on the 11.3, 20.7, 23.7, 37, and 42-ev resonances gave Γ_γ's of 40±20, 160±50, 70±20, 90±30, and 80±30 mv. The data and results are summarized in Table IX, based on a Γ_γ of 70±20 mv. Since the sample thickness (n) is given for the element, the neutron widths listed are less than the true values. Thus the neutron width listed in Table IX for a particular resonance would be increased by a factor of (1/0.976) if the resonance were assigned to Lu^{175} and by a factor of (1/0.024) if assigned to Lu^{176}.

In addition to the 5 resonances previously reported[14] from 4 to 21 ev, five additional resonances were observed. The thick and thin measurements on the 57-ev resonance indicate that it is not a single resonance. If we assume that resonances with $\Gamma_n^0<0.1$ mv are in Lu^{176}, there are 13 resonances below 45 ev in Lu^{175} and D equals 7±2 ev for Lu^{175}. The ratio $\bar{\Gamma}_n^0/D$ for Lu^{175} equals $(1.7\pm0.2)\times10^{-4}$. Since many resonances in Lu^{176} must have been masked by Lu^{175} resonances, no level spacing for Lu^{176} is given.

Hafnium ($_{72}$Hf).—Four thick samples of HfO_2 (~1 g/cm²) enriched to 61.0 percent Hf^{177}, 80.9 percent Hf^{178}, 46.6 percent Hf^{179}, and 93.96 percent Hf^{180} were run from 4 to 150 ev with a resolution of 0.07 μsec/m. A thick sample (~4 g/cm²) of normal hafnium metal was also run in the same energy range. The two low-energy resonances in Hf^{177} at 1.08 and 2.38 ev were not measured. Since only 14 mg of 7.85 percent Hf^{174} and only 58 mg of 48.46 percent Hf^{176} were available, only thin samples of these isotopes could be measured. In order to get thin runs on the 7.8-ev resonance, samples of Zr containing 2 percent Hf were used as well as thin samples enriched in other isotopes. The data and results are summarized in Table X based on a Γ_γ of 56±15 mv for Hf^{177} and 60±20 mv for the other isotopes. The resonances and their assignments are in agreement with Argonne work,[22] in which resonances up to 13 ev were measured. In this work a Γ_γ of 43±10 mv and a $2g\Gamma_n$ of 1.8±0.5 mv were found for the 1.08-ev resonance. Recent work by Levin[23] gives a Γ_γ of 63±8 mv and a $2g\Gamma_n$ of 6.8±0.6 mv for the 2.38-ev resonance, and a Γ_γ of 44±20 mv and a $2g\Gamma_n$ of 11±2 mv for the 6.5-ev resonance.

[22] Bollinger, Harris, Hibdon, and Muehlhause, Phys. Rev. **92**, 1527 (1953).
[23] J. S. Levin (to be published).

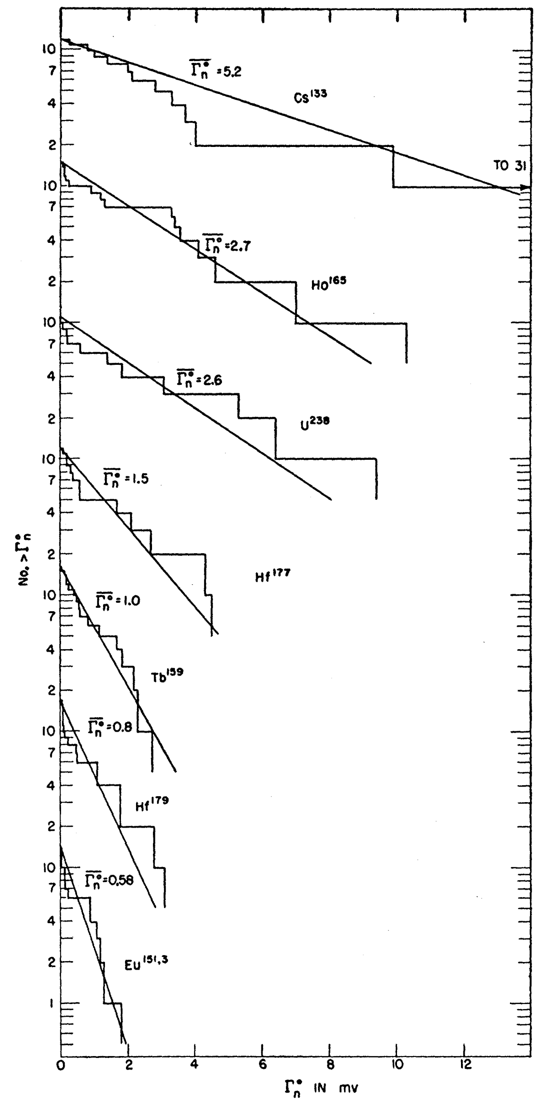

FIG. 7. The distribution in size of the reduced neutron widths for various nuclides, plotted in the same manner as Fig. 4. The slopes of the straight lines are computed from the arithmetic averages of the neutron widths.

The 12 resonances in Hf^{177} found below 34 ev give a D of 5.6±0.6 ev. Their size distribution is given in Fig. 7. The ratio $\bar{\Gamma}_n^0/D$ for Hf^{177} is $(3.0\pm0.4)\times10^{-4}$. In Hf^{179} the wide spacing of the first few levels and the large number of small levels from 50–65 ev (see Fig. 7) complicates the determination of D, with a resulting value of 8±2 ev, somewhat less accurate than expected from the number of levels found. The ratio $\bar{\Gamma}_n^0/D$ is $(1.3\pm0.3)\times10^{-4}$. There is only one resonance in Hf^{178} and one in Hf^{180} up to 100 ev. One resonance was found in Hf^{174}, but since only a thin sample was available small resonances may have been missed. No resonances were found in Hf^{176}, but again since only a thin sample of enriched Hf^{176} was available small resonances would not have been detected.

TABLE VI. Neutron widths of resonances of the isotopes of europium ($_{63}$Eu) based on a Γ_γ of 90±20 mv. The two isotopes are assumed to be equally abundant in computing $1/n$.

E_0 (ev)	Δ (ev)	$(1/n)\times10^{24}$ (cm²/atom)	Area (% error) (ev)	Γ_n (% error) (mv)	r	Weighted Γ_n (mv)	Reduced width Γ_n^0 (mv)
4.83±0.04	0.057	1420	0.015 (30)	0.051 (30)	<0.1	0.048±0.008	0.022±0.004
		322	0.056 (20)	0.047 (21)	<0.1		
5.47±0.05	0.061	1420	0.036 (20)	0.142 (20)	<0.1	0.133±0.018	0.057±0.008
		322	0.121 (15)	0.126 (18)	0.2		
6.03±0.08	0.064	7700	0.015 (25)	0.35 (25)	<0.1	0.35±0.05	0.14±0.02
		5000	0.030 (40)	0.46 (42)	<0.1		
		1420	0.080 (30)	0.37 (33)	0.1		
		322	0.17 (30)	0.20 (37)	0.1		
6.25±0.08	0.065	7700	0.017 (25)	0.43 (23)	<0.1	0.41±0.07	0.16±0.03
		5000	0.030 (40)	0.47 (40)	<0.1		
		1420	0.080 (30)	0.39 (33)	<0.1		
		322	0.24 (30)	0.35 (44)	0.2		
7.24±0.10	0.070	7700	0.065 (30)	2.0 (33)	<0.1	2.4±0.5	0.89±0.18
		5000	0.13 (25)	2.7 (30)	0.1		
		1420	0.30 (20)	2.4 (33)	0.3		
7.47±0.10	0.071	7700	0.065 (30)	2.0 (33)	<0.1	2.4±0.5	0.88±0.18
		5000	0.13 (25)	2.7 (30)	0.1		
		1420	0.30 (20)	2.5 (34)	0.3		
8.90±0.09	0.078	7700	0.090 (12)	3.4 (14)	0.1	4.2±0.4	1.41±0.14
		5000	0.19 (15)	5.4 (19)	0.1		
		1420	0.38 (7)	4.3 (18)	1.0		
10.5±0.1	0.085	7700	0.025 (30)	1.0 (32)	<0.1	1.90±0.13	0.59±0.04
		5000	0.075 (10)	2.14 (10)	<0.1		
		1420	0.192 (7)	1.81 (9)	0.3		
11.1±0.2	0.087	1420	0.060 (40)	0.5 (43)	<0.1	0.5±0.2	0.15±0.06
11.7±0.1	0.089	7700	0.061 (20)	3.0 (22)	<0.1	3.7±0.3	1.08±0.08
		5000	0.121 (10)	4.0 (11)	0.3		
		1420	0.30 (10)	3.7 (18)	0.5		
12.3±0.2	0.091	7700	0.018 (50)	0.9 (51)	<0.1	1.2±0.2	0.34±0.07
		5000	0.045 (30)	1.4 (30)	<0.1		
		1420	0.106 (25)	1.1 (29)	<0.1		
12.7±0.1	0.093	7700	0.020 (50)	1.0 (49)	<0.1	2.2±0.4	0.62±0.12
		5000	0.082 (20)	2.9 (20)	<0.1		
		1420	0.169 (15)	1.9 (17)	0.2		
13.6±0.2	0.096	1420	0.04 (50)	0.4 (53)	<0.1	0.4±0.2	0.11±0.06
14.8±0.2	0.10	7700	0.020 (50)	1.1 (51)	<0.1	1.9±0.3	0.49±0.07
		5000	0.056 (20)	2.2 (21)	<0.1		
		1420	0.150 (15)	1.8 (19)	0.2		
15.2±0.2	0.10	7700	0.039 (50)	2.3 (53)	<0.1	2.2±0.3	0.57±0.08
		5000	0.057 (20)	2.3 (20)	<0.1		
		1420	0.157 (15)	2.0 (18)	0.2		

Tantalum ($_{73}Ta^{181}$).—Two thick samples (7.80 and 0.89 g/cm²) of tantalum metal were measured from 7 to 150 ev with a resolution of 0.07 μsec/m. Two thin samples (0.0496 and 0.296 g/cm²) were run from 7 to 45 ev only. The 4.3-ev resonance was not measured since this resonance has been studied recently by the BNL crystal spectrometer group,[24] giving $\Gamma_\gamma=49\pm6$ mv and $2g\Gamma_n=4.3\pm0.7$ mv. The data are summarized in Table XI based on a Γ_γ of 50±10 mv. Thick and thin runs on the 10.4, 13.95, and 20.5-ev resonances give Γ_γ's of 49±11, 55±13, and 49±15 mv. Several resonances of Table XI below 40 ev had not been found in earlier work[25,26] in this energy range. For example, the previously reported resonances at 24 and 35 ev have each been resolved into two resonances, as was already shown in unpublished work by the MTR fast-chopper group at Arco, Idaho. A small resonance reported[27] at about 11 ev was not found in our work. The 10 resonances below 45 ev give a D of 9.0±1.0 ev. The $\bar{\Gamma}_n^0/D$ ratio is $(1.8\pm0.3)\times10^{-4}$.

Uranium ($_{92}U^{238}$).—The transmissions of eight different thicknesses (from 0.0266 to 36.0 g/cm²) of normal uranium were measured in various energy regions from 5 to 750 ev with a resolution of 0.07 μsec/m. Above 200 ev, however, only a single sample thickness of 18.0 g/cm² was used. A 12.0-g/cm² sample was run from 5 to 200 ev, as well as various thin samples. For example, in

[24] R. E. Wood (private communication).
[25] Melkonian, Havens, and Rainwater, Phys. Rev. **92**, 702 (1953).
[26] R. L. Christensen, Phys. Rev. **92**, 1509 (1953).
[27] Gaerttner, Yeater, and Albert, Knolls Atomic Power Laboratory Report KAPL-1084, March, 1954 (unpublished).

TABLE VI.—*Continued.*

E_0 (ev)	Δ (ev)	$(1/n)\times10^{24}$ (cm²/atom)	Area (% error) (ev)	Γ_n (% error) (mv)	r	Weighted Γ_n (mv)	Reduced width Γ_n^0 (mv)
16.8±0.2	0.11	7700	0.028 (50)	1.8 (51)	<0.1	1.5±0.2	0.37±0.05
		5000	0.045 (15)	1.9 (17)	<0.1		
		1420	0.093 (10)	1.2 (10)	<0.1		
18.0±0.2	0.11	7700	0.058 (25)	4.1 (25)	<0.1	5.0±0.5	1.18±0.13
		5000	0.106 (15)	5.2 (17)	<0.1		
		1420	0.287 (10)	5.2 (15)	0.4		
18.8±0.2	0.11	7700	0.030 (50)	2.2 (50)	<0.1	3.9±0.8	0.90±0.18
		5000	0.069 (30)	3.4 (31)	<0.1		
		1420	0.25 (20)	4.5 (25)	0.2		
19.3±0.2	0.11	7700	0.060 (30)	4.6 (32)	<0.1	4.3±0.8	0.98±0.19
		5000	0.069 (30)	3.5 (33)	<0.1		
		1420	0.25 (20)	4.6 (26)	0.2		
20.1±0.2	0.11	7700	0.110 (20)	9.3 (23)	<0.1	11.5±1.2	2.6±0.3
		5000	0.212 (7)	12.8 (10)	0.3		
		1420	0.42 (10)	10.0 (21)	0.6		
22.0±0.3	0.12	7700	0.037 (35)	3.2 (34)	<0.1	2.9±0.7	0.62±0.15
		1420	0.15 (30)	2.7 (34)	<0.1		
22.5±0.3	0.12	7700	0.060 (30)	5.3 (32)	<0.1	6.7±1.3	1.4±0.3
		5000	0.12 (25)	7.3 (30)	<0.1		
		1420	0.32 (20)	7.2 (28)	0.2		
24.1±0.3	0.13	7700	0.034 (40)	3.2 (42)	<0.1	3.0±0.8	0.61±0.15
		3460	0.068 (30)	2.9 (31)	<0.1		
25.0±0.3	0.13	7700	0.061 (30)	5.9 (31)	<0.1	5.8±1.2	1.2±0.3
		3460	0.12 (25)	5.7 (29)	<0.1		
27.0±0.4	0.14	3460	0.14 (25)	7.1 (28)	<0.1	6.7±1.4	1.3±0.3
		7700	0.061 (30)	6.5 (31)	<0.1		
29.5±0.4	0.14	3460	0.057 (50)	2.9 (52)	<0.1	2.9±1.5	0.5±0.3
30.8±0.4	0.14	3460	0.064 (50)	3.5 (52)	<0.1	3.5±1.8	0.6±0.3
31.8±0.4	0.15	3460	0.059 (50)	3.3 (52)	<0.1	3.3±1.7	0.6±0.3
35.1±0.5	0.16	3460	0.11 (30)	6 (33)	<0.1	6±2	1.0±0.3
36.9±0.5	0.16	3460	0.17 (30)	12 (33)	<0.1	12±4	2.0±0.7
38.3±0.6	0.16	3460	0.17 (30)	13 (34)	<0.1	13±4	2.1±0.7
42.2±0.7	0.17	3460	0.25 (25)	22 (32)	<0.1	22±7	3.4±1.1
47.4±0.8	0.18	3460	0.38 (20)	41 (30)	0.1	41±12	6±2

addition to the 12.0-g/cm² run, measurements were made on the 66.5-ev resonance with three other samples, of thicknesses 4.66, 0.925, and 0.123 g/cm². Two 36.0-g/cm² samples were run in the region of 90 ev to obtain data on the extremely weak resonance at 90 ev. A minor correction to the transmission was made for the U^{235} content when necessary.

The results are summarized in Table XII. The data on the 6.70-ev resonance were obtained from Levin[23] and are included for completeness. The measurements on the first four resonances are sufficiently accurate to give good results for Γ and hence Γ_γ. The Γ's obtained are 25.5±2.0, 33±5, 61±7, and 44±10 mv for the 6.7, 21, 37, and 66.5-ev resonances, respectively, hence the Γ_γ's are 24±2, 25±5, 29±9, and 17±10 mv. These values are all consistent with a single Γ_γ of 25 mv. Table XII summarizes the data based on a Γ_γ of 25±5 mv for all resonances, except the 6.7-ev resonance for which a Γ_γ of 24±2 mv was used.

There are eleven resonances up to 200 ev giving a D of 18±2 ev. The size distribution of their neutron widths is shown in Fig. 7. It is interesting that the ratio of the largest to the smallest reduced neutron width is about 10^3. Any resonance up to 100 ev with a Γ_n^0 of 1/500 of the average Γ_n^0 would have been found, as well as any resonance 1/100 of the average Γ_n^0 in the 100–200-ev range. Above 200 ev it is apparent that small resonances may have been missed or that some resonances listed may be two resonances. The ratio $\bar{\Gamma}_n^0/D$ up to 400 ev is $(1.2\pm0.2)\times10^{-4}$. The "resonance absorption integral," $\int\sigma_a dE/E$, where σ_a is the absorption cross section, is given by $\sum \pi\sigma_0\Gamma_\gamma/2E_0$ over the resonances. The value calculated from the resonances up to 420 ev is 265±12 b. As the additional contribution for the resonances above 420 ev (calculated from the average resonance parameters) amounts to 11±3 b, the resonance absorption integral is 276±12 b.

IV. DISCUSSION OF RESULTS

We have seen in the preceding section that the experimental total cross sections give the level spacings directly by a simple counting of levels, with an accuracy limited

TABLE VII. Neutron widths of resonances in terbium ($_{65}Tb^{159}$) based on a Γ_γ of 90±30 mv.

E_0 (ev)	Δ (ev)	$(1/n)\times10^{24}$ (cm²/atom)	Area (% error) (ev)	Γ_n (% error) (mv)	r	Weighted Γ_n (mv)	Reduced width Γ_n^0 (mv)
3.35±0.03	0.046	1290 499	0.158 (7) 0.30 (6)	0.43 (14) 0.43 (23)	0.7 1.7	0.43±0.05	0.24±0.03
4.99±0.05	0.057	1290 499	0.022 (23) 0.036 (14)	0.072 (25) 0.045 (16)	<0.1 <0.1	0.055±0.008	0.025±0.004
11.14±0.10	0.085	1290 499	0.512 (5) 0.93 (5)	7.4 (25) 11.4 (30)	1.9 2.1	9.2±1.8	2.8±0.6
14.4±0.2	0.096	499	0.131 (16)	0.54 (20)	0.2	0.54±0.11	0.14±0.03
21.4±0.2	0.12	1290 499	0.151 (12) 0.240 (12)	2.4 (15) 1.7 (17)	0.1 0.2	2.1±0.2	0.46±0.05
24.7±0.3	0.13	1290 499	0.272 (8) 0.50 (10)	5.7 (14) 6.0 (24)	0.3 0.7	5.8±0.7	1.17±0.14
27.8±0.3	0.13	499 252	0.108 (13) 0.24 (18)	0.82 (15) 1.08 (24)	<0.1 0.2	0.90±0.12	0.17±0.02
34.1±0.4	0.15	1290 499 252	0.160 (17) 0.244 (9) 0.52 (14)	4.0 (21) 2.6 (13) 4.2 (27)	<0.1 0.2 0.4	3.3±0.7	0.57±0.11
44.2±0.6	0.17	1290 499 252	0.16 (23) 0.34 (12) 0.63 (15)	5.3 (27) 5.1 (18) 7.3 (35)	<0.1 0.2 0.3	5.6±0.8	0.84±0.13
46.6±0.6	0.17	1290 499 252	0.45 (12) 0.51 (9) 0.88 (11)	21 (20) 9.7 (17) 16 (32)	0.3 0.5 0.7	15±3	2.2±0.4
51.1±0.7	0.18	499 252	0.21 (19) 0.47 (20)	3.1 (24) 4.7 (33)	<0.1 0.2	3.7±0.7	0.52±0.10
54.9±0.7	0.19	252	0.19 (30)	1.6 (36)	<0.1	1.6±0.6	0.21±0.08
58.7±0.8	0.20	499 252	0.26 (30) 0.43 (25)	4.5 (37) 4.6 (37)	<0.1 0.1	4.6±1.1	0.60±0.14
66.1±1.1	0.21	499 252	0.45 (15) 1.04 (13)	11 (22) 31 (33)	0.2 0.6	15±4	1.9±0.5
74.6±1.3	0.22	499 252	0.60 (17) 1.04 (25)	18 (28) 30 (60)	0.2 0.2	20±5	2.3±0.6
78.2±1.4	0.23	499 252	0.47 (18) 0.92 (30)	13 (26) 23 (74)	0.1 0.2	15±4	1.7±0.4
91.9±1.8	0.24	499 252	0.60 (20) 1.00 (18)	22 (31) 29 (40)	0.2 0.3	24±6	2.5±0.7
97.9±1.9	0.25	499 252	0.76 (18) 1.48 (15)	34 (30) 65 (33)	0.2 0.5	45±11	4.5±1.1
112.5±2.0	0.27	499 252	0.94 (30) 1.6 (25)	53 (53) 80 (56)	0.1 0.2	65±25	6.0±2.5
115±2	0.27	499 252	0.95 (30) 1.7 (25)	55 (53) 90 (55)	0.1 0.2	70±30	7±3
122±3	0.28	252	1.2 (30)	50 (70)	0.1	50±30	4±3
131±3	0.29	252	0.65 (35)	16 (50)	<0.1	16±8	1.4±0.7
144±3	0.30	499 252	1.08 (22) 2.5 (20)	80 (36) 180 (35)	0.2 0.5	120±30	10±3
156±4	0.32	499 252	1.03 (26) 2.8 (15)	80 (44) 230 (30)	0.2 0.7	160±40	13±3

primarily by the small number of levels observed, but affected also by the possibility of loss of levels by poor resolution. The reduced neutron widths (rather $2g\Gamma_n^0$) that are obtained are subject not only to experimental error but to uncertainty arising from lack of knowledge of Γ_γ for the individual levels. Although the lack of knowledge of Γ_γ at first sight seems serious, the final uncertainty is usually the experimental error itself, because of the weak dependence of $2g\Gamma_n^0$ on Γ_γ for average sample thicknesses. For comparison with theory, the reduced neutron width Γ_n^0 rather than $2g\Gamma_n^0$ is needed, and hence there is additional uncertainty for all but zero-spin target nuclei because $2g$ is not unity, in the worst case (spin-$\frac{1}{2}$ target nuclei) the two possible values being $\frac{1}{2}$ and $\frac{3}{2}$.

In spite of the limitation arising from the g value, several interesting features are clearly revealed by a survey of the measured neutron widths. The values that

TABLE VIII. Neutron width of resonances in holmium ($_{67}Ho^{165}$) based on a Γ_γ of 90±20 mv.

E_0 (ev)	Δ (ev)	$(1/n)\times10^{24}$ (cm²/atom)	Area (% error) (ev)	Γ_n (% error) (mv)	r	Weighted Γ_n (mv)	Reduced width Γ_n^0 (mv)
3.92±0.03	0.050	1470	0.406 (4)	2.5 (18)	1.8	2.5±0.5	1.3±0.2
12.8±0.1	0.089	1470	0.561 (3.3)	13.1 (16)	1.7	13.1±1.8	3.4±0.5
18.2±0.2	0.11	1470 72	0.050 (25) 0.61 (7)	0.69 (28) 1.11 (22)	<0.1 1.1	0.92±0.17	0.22±0.04
21.3±0.2	0.12	72	0.48 (7)	0.73 (16)	0.7	0.73±0.12	0.16±0.03
35.9±0.4	0.15	1470 72	0.25 (15) 1.07 (6)	8.4 (19) 6.4 (22)	0.1 1.3	7.5±1.1	1.20±0.18
37.9±0.5	0.15	72	0.22 (16)	0.36 (20)	<0.1	0.36±0.07	0.059±0.012
40.3±0.5	0.16	1470 72	0.48 (12) 1.75 (7)	23 (19) 19 (22)	0.3 1.1	21±3	3.3±0.5
48.5±0.6	0.17	1470 72	0.47 (11) 1.77 (8)	26 (18) 22 (25)	0.2 0.9	25±4	3.6±0.5
52.2+0.7	0.18	1470 72	0.73 (6) 2.26 (11)	55 (13) 34 (26)	0.6 0.7	51±6	7.0±0.8
55.3±0.8	0.19	72	0.96 (17)	6.6 (46)	0.3	7±3	0.9±0.4
66.3±1.1	0.20	1470 72	0.51 (12) 1.74 (11)	38 (19) 38 (26)	0.2 0.6	38±6	4.6±0.7
70.0±1.2	0.210	72	0.34 (30)	1.1 (38)	<0.1	1.1±0.4	0.13±0.04
73.1±1.3	0.21	1470 72	0.42 (17) 2.03 (9)	30 (25) 38 (22)	<0.1 0.7	35±6	4.1±0.7
83.4±1.5	0.23	72	0.32 (35)	1.2 (46)	<0.1	1.2±0.6	0.13±0.06
87.2±1.6	0.23	1470 72	0.73 (13) 3.72 (8)	79 (18) 108 (13)	0.2 0.6	96±10	10.3±1.1
96±2	0.24	1470 72	0.99 (11) 3.9 (9)	133 (18) 119 (14)	0.2 0.6	125±15	12.7±1.5
104±2	0.26	1470 72	0.52 (20) 2.7 (13)	54 (27) 75 (24)	<0.1 0.4	65±13	6.4±1.3
123±3	0.28	72	1.66 (18)	34 (45)	0.3	34±16	3.1±1.5
130±3	0.29	1470 72	0.79 (24) 4.7 (10)	110 (32) 180 (15)	<0.1 0.4	160±25	14±2

have been obtained in the present study reveal that Γ_n^0 varies over an extremely large range, a fact that lessens greatly the disadvantage of the g uncertainty simply because the values range over a much greater spread than results from the two possible g values. Of the many possible aspects of the statistics of level parameters that could be studied, only a few prominent characteristics will be discussed at present, omitting possible trends that cannot be delineated clearly at the present time because of insufficient data. The neutron widths will be considered first, then the level spacings, and finally the ratio $\bar{\Gamma}_n^0/\bar{D}$ which has an important bearing on current nuclear models.

A. Neutron Widths

The neutron width of a level is related to the mean lifetime τ_n of the state relative to disintegration by emission of a neutron by the relationship,

$$\Gamma_n=\hbar/\tau_n. \tag{5}$$

The width can be considered crudely as being determined by the time required for concentration of the excitation energy on a particular neutron and by the probability that this neutron will penetrate the nuclear potential barrier. Thus the width Γ_n and the reduced width Γ_n^0 are given by

$$\Gamma_n=\hbar p/t_0,\qquad \Gamma_n^0=\hbar p^0/t_0, \tag{6}$$

where t_0 is the lifetime spent by the nucleus in the particular excitation state before the energy is concentrated on a single neutron, p is the actual barrier penetrability, and p^0 is the value for a 1-ev neutron.

As the barrier penetrability p^0 is expected to be practically the same from one level to another in a particular nucleus, the wide range in neutron widths observed must indicate a corresponding wide range of lifetimes for the individual nuclear states. As we shall see later, the barrier penetration (given by $2\pi\bar{\Gamma}_n^0/D$) is of the order of 10^{-3} for the elements considered; hence the intrinsic nuclear lifetime, t_0, varies from about 10^{-13} to 10^{-16} sec for the observed range in Γ_n^0 of 0.01 mv to 10 mv. In spite of this wide range, the values of t_0 are always much greater than the time required for a nucleon to cross the nucleus, which is about 10^{-21} second. The wide range in t_0 observed reflects the differences

TABLE IX. Neutron widths of resonances in lutetium ($_{71}$Lu) based on a Γ_γ of 70±20 mv. The sample thickness $(1/n)$ is the atomic value (see text).

E_0 (ev)	Δ (ev)	$(1/n)\times10^{24}$ (cm²/atom)	Area (% error) (ev)	Γ_n (% error) (mv)	r	Weighted Γ_n (mv)	Reduced width Γ_n^0 (mv)
4.39±0.03	0.051	171	0.032 (35)	0.012 (47)	<0.1	0.012±0.006	0.006±0.003
4.78±0.03	0.053	980	0.10 (8)	0.28 (11)	0.4	0.28±0.03	0.128±0.014
		171	0.36 (15)	0.33 (33)	0.7		
5.22±0.04	0.056	980	0.285 (7)	1.3 (22)	1.4	1.2±0.2	0.52±0.09
		171	0.56 (15)	0.9 (36)	0.9		
6.17±0.05	0.060	980	0.022 (30)	0.081 (33)	<0.1	0.062±0.012	0.025±0.005
		171	0.080 (23)	0.047 (27)	0.1		
9.8±0.1	0.076	72.5	0.11 (22)	0.044 (26)	0.2	0.044±0.012	0.014±0.004
11.3±0.1	0.082	980	0.34 (7)	3.4 (18)	1.2	3.2±0.5	0.95±0.15
		72.5	1.04 (8)	2.8 (30)	1.8		
14.1±0.1	0.091	980	0.82 (5)	22 (19)	1.7	18±3	4.8±0.7
		72.5	2.00 (12)	12 (28)	1.0		
15.5±0.2	0.095	980	0.157 (8)	1.46 (11)	0.3	1.40±0.15	0.35±0.04
		72.5	0.54 (20)	0.9 (44)	0.5		
20.0±0.2	0.11	72.5	0.095 (20)	0.08 (25)	<0.1	0.08±0.02	0.018±0.005
20.7±0.2	0.11	980	0.161 (10)	2.0 (13)	<0.1	2.3±0.3	0.51±0.07
		72.5	0.92 (7)	3.6 (30)	1.5		
22.0±0.2	0.12	72.5	0.082 (24)	0.07 (29)	<0.1	0.07±0.02	0.015±0.004
23.7±0.2	0.12	980	0.29 (8)	5.0 (14)	0.6	4.9±0.7	1.01±0.14
		72.5	1.00 (7)	4.6 (29)	1.7		
24.8±0.3	0.12	72.5	0.15 (28)	0.17 (34)	<0.1	0.17±0.06	0.034±0.012
27.3±0.3	0.13	72.5	0.22 (22)	0.27 (30)	<0.1	0.27±0.08	0.052±0.016
28.2±0.3	0.13	980	0.090 (21)	1.4 (26)	<0.1	1.4±0.3	0.26±0.05
		72.5	0.56 (14)	1.4 (40)	0.6		
30.4±0.3	0.13	980	0.39 (11)	9.7 (20)	0.4	9.2±1.7	1.7±0.3
		72.5	1.11 (16)	7.4 (40)	0.7		
31.2±0.3	0.14	980	0.122 (22)	2.1 (30)	<0.1	2.3±0.6	0.41±0.10
		72.5	0.75 (20)	3.0 (50)	0.5		
37.1±0.4	0.15	980	0.26 (12)	6.2 (16)	0.2	6.4±0.9	1.05±0.14
		72.5	1.02 (9)	7.0 (30)	1.2		
41.5±0.5	0.16	980	0.59 (7)	22 (15)	1.0	24±3	3.7±0.4
		72.5	1.96 (7)	27 (18)	1.3		
46.2±0.6	0.17	72.5	0.20 (32)	0.39 (39)	<0.1	0.39±0.15	0.06±0.02
50.7±0.7	0.17	980	0.68 (6)	37 (14)	0.7	38±4	5.3±0.6
		72.5	2.25 (6)	39 (16)	1.1		
54.3±0.7	0.18	72.5	0.32 (28)	0.8 (39)	0.1	0.8±0.3	0.11±0.04
57.5±1.0 (2 equal resonances)	0.18	980	0.10 (20)	3.1 (23)	<0.1	{3.7±0.7	0.49±0.09
		72.5	0.77 (10)	4.6 (26)	0.4	{3.7±0.7	0.49±0.09
63.0±1.0	0.19	72.5	0.39 (31)	1.3 (45)	<0.1	1.3±0.6	0.16±0.08
71.0±1.2	0.21	72.5	1.03 (10)	10 (30)	0.9	10±3	1.2±0.4
86.0±1.5	0.23	72.5	0.67 (25)	4 (50)	0.2	4±2	0.4±0.2
89.4±1.6	0.23	72.5	0.69 (25)	4 (50)	0.2	4±2	0.4±0.2
98.9±1.8	0.25	980	0.87 (17)	80 (30)	0.2	93±11	9.3±1.1
		72.5	3.1 (10)	97 (13)	0.5		
104±2	0.25	980	0.50 (30)	37 (45)	<0.1	36±11	3.5±1.1
		72.5	1.6 (18)	35 (32)	0.4		
110±2	0.26	980	0.53 (25)	41 (37)	<0.1	39±10	3.7±0.9
		72.5	1.70 (17)	38 (30)	0.5		
119±3	0.27	980	0.57 (25)	52 (38)	<0.1	83±11	7.6±1.0
		72.5	2.8 (11)	89 (13)	0.5		
132±3	0.28	980	1.17 (14)	148 (20)	0.2	150±15	13.1±1.3
		72.5	3.9 (10)	150 (11)	0.5		

TABLE X. Neutron widths of resonances in the isotopes of hafnium ($_{72}$Hf) based on a Γ_γ of 56±15 mv for Hf^{177} and 60±20 for the other isotopes.

Isotope	E_0 (ev)	Δ (ev)	Sample	$(1/n)\times10^{24}$ (cm²/atom)	Area (% error) (ev)	Γ_n (% error) (mv)	r	Weighted Γ_n (mv)	Reduced width Γ_n^0 (mv)
Hf^{174}	30.5±0.4	0.135	174	41 000	0.135 (20)	49 (24)	<0.1	49±6	8.9±1.2
			Normal	57 000	0.101 (15)	49 (16)	<0.1		
Hf^{177}	5.9±0.1	0.057	177	1080	0.48 (10)	5.1 (29)	1.2	5.1±1.5	2.1±0.6
	6.6±0.1	0.061	177	1080	0.66 (10)	11 (29)	0.9	11±3	4.3±1.3
	8.8±0.1	0.070	177	1080	0.49 (20)	7.5 (41)	0.6	8±3	2.7±1.1
	13.7±0.2	0.090	177	543	0.139 (11)	0.70 (13)	0.2	0.67±0.08	0.18±0.02
			Normal	537	0.128 (13)	0.62 (17)	0.2		
	14.1±0.2	0.090	177	543	0.30 (10)	2.2 (18)	0.4	2.2±0.3	0.59±0.08
			Normal	537	0.31 (10)	2.2 (18)	0.4		
	22.2±0.2	0.12	177	543	0.29 (11)	2.6 (19)	0.4	2.7±0.3	0.57±0.06
			Normal	537	0.295 (6)	2.7 (13)	0.6		
	23.5±0.2	0.12	177	543	0.20 (16)	1.6 (22)	0.1	1.6±0.4	0.33±0.07
	25.9±0.3	0.12	177	543	0.056 (17)	0.41 (19)	<0.1	0.41±0.08	0.08±0.02
	27.2±0.3	0.13	177	543	0.193 (8)	1.80 (10)	0.4	1.80±0.18	0.35±0.04
	33.2±0.4	0.14	177	543	0.121 (17)	1.2 (20)	<0.1	1.2±0.2	0.21±0.04
	37.2±0.5	0.15	177	543	0.75 (11)	23 (21)	0.6	23±5	3.8±0.8
	43.6±0.6	0.16	177	543	0.271 (8)	4.3 (12)	0.3	4.3±0.5	0.65±0.08
	45.7±0.6	0.16	177	543	0.28 (9)	4.6 (14)	0.2	4.6±0.6	0.68±0.10
	46.8±0.6	0.16	177	543	0.29 (10)	4.9 (17)	0.2	4.9±0.8	0.72±0.12
	49.4±0.7	0.17	177	543	1.10 (4)	55 (8)	1.0	55±5	7.8±0.6
	55.6±0.7	0.18	177	543	0.58 (9)	18 (21)	0.4	18±4	2.4±0.5
	57.2±0.8	0.18	177	543	0.50 (10)	13 (20)	0.4	13±3	1.7±0.3
	60.3±1.0	0.19	177	543	0.15 (25)	2.8 (30)	<0.1	2.8±0.8	0.36±0.11
	64.4±1.0	0.19	177	543	1.12 (5)	66 (11)	0.7	66±8	8.2±0.9
	67.7±1.1	0.20	177	543	0.79 (5)	36 (11)	0.7	36±4	4.4±0.5
	72.3±1.2	0.21	177	543	0.46 (15)	14 (26)	0.1	14±4	1.6±0.4
	77.2±1.3	0.21	177	543	0.48 (9)	16 (17)	0.2	16±3	1.8±0.3
	84.3±1.5	0.22	177	543	0.14 (25)	3.4 (28)	<0.1	3.4±0.9	0.37±0.10
	86.2±1.6	0.22	177	543	0.57 (9)	22 (18)	0.3	22±4	2.4±0.5
	93.6±1.8	0.23	177	543	0.22 (17)	6.4 (20)	<0.1	6.4±1.3	0.66±0.13
	98.5±1.9	0.24	177	543	0.37 (13)	13 (19)	<0.1	13±3	1.3±0.3
	103±2	0.25	177	543	0.47 (20)	20 (33)	<0.1	20±7	2.0±0.7
	105±2	0.25	177	543	0.65 (18)	32 (31)	0.1	32±10	3.1±1.0

in intrinsic properties of individual nuclear levels; hence some information can be obtained from the data on the nature of the distribution of the nuclear lifetimes, or more simply, as they are expressed by the reduced neutron widths. As already mentioned in connection with the discussion of thulium, the observed reduced neutron widths follow an exponential distribution as a function of size. Distributions similar to that shown in Sec. III for thulium have been found for other nuclides as well. In order to compare the distributions observed for various nuclides, the actual results for all cases in which at least 11 levels were observed are exhibited together in Fig. 7. While it is certainly true that the exponential distribution is a good approximation for the observations, it is not definitely established that this law is followed exactly.

The effect of lack of knowledge of g on the Γ_n^0 distribution was discussed in Sec. III A for the case of thulium where it was shown that equal spacings for the two spin states would give a curve concave upward when plotted as in Fig. 7, even if the exponential is strictly true for the levels of each spin state. If, on the other hand, the levels with higher g (thus higher compound nuclear spin J) should have a smaller level spacing, the g effect might cancel (it would exactly if the level spacing contains a $2J+1$ factor, see Sec. IV B). Some of the distribution curves are slightly concave upward and this behavior might be related to the g effect. However, in the light of the present limited amount of data, the exponential distribution holds surprisingly well, and seems firmly enough established to justify theoretical calculations. The distribution law of neutron widths has not been treated extensively in any published theory of nuclear level structure as yet.

TABLE X.—*Continued.*

Isotope	E_0 (ev)	Δ (ev)	Sample	$(1/n)\times10^{24}$ (cm²/atom)	Area (% error) (ev)	Γ_n (% error) (mv)	r	Weighted Γ_n (mv)	Reduced width Γ_n^0 (mv)
Hf^{178}	7.80±0.10	0.070	Zr	165 000	0.151 (7)	57 (9)	0.4	49±3	17.5±1.0
			Zr	190 000	0.117 (10)	49 (12)	0.2		
			179	8000	0.82 (5)	46 (13)	1.6		
			180	9300	0.71 (5)	41 (14)	2.0		
			Normal	2710	1.45 (5)	50 (13)	1.8		
Hf^{179}	5.69±0.05	0.056	179	1150	0.437 (5)	4.2 (32)	2.5	4.2±1.3	1.8±0.6
	17.8±0.2	0.10	179	324	0.307 (6)	1.5 (16)	1.1	2.0±0.2	0.47±0.05
			Normal	736	0.257 (8)	2.5 (15)	0.7		
	24.0±0.2	0.12	179	324	0.535 (5)	5.3 (25)	1.7	5.3±1.4	1.1±0.3
	27.0+0.3	0.12	179	324	0.216 (10)	1.25 (15)	0.3	1.25±0.19	0.24±0.04
	31.5±0.4	0.13	179	324	0.51 (6)	6.0 (21)	1.3	6.0±1.2	1.1±0.2
	36.8±0.5	0.15	179	324	0.80 (10)	17 (29)	0.9	17±5	2.8±0.8
	40.6±0.5	0.15	179	324	0.86 (5)	20 (20)	1.8	20±4	3.1±0.6
	42.8±0.6	0.16	179	324	0.68 (7)	13.1 (21)	1.0	11.9±1.7	1.8±0.2
			179	324	0.63 (4)	10.8 (18)	1.5		
	44.7±0.6	0.16	179	324	0.055 (25)	0.41 (27)	<0.1	0.41±0.12	0.06±0.02
	48.1±0.7	0.17	179	324	0.093 (25)	0.8 (30)	<0.1	0.8±0.2	0.12±0.03
	51.1±0.7	0.17	179	324	0.103 (20)	0.9 (22)	<0.1	0.9±0.2	0.13±0.03
	51.7±0.7	0.17	179	324	0.059 (20)	0.51 (20)	<0.1	0.51±0.10	0.07±0.02
	52.4±0.7	0.17	179	324	0.060 (20)	0.53 (20)	<0.1	0.53±0.10	0.07±0.02
	53.5±0.7	0.18	179	324	0.062 (20)	0.56 (21)	<0.1	0.56±0.12	0.08±0.02
	55.4±0.8	0.18	179	324	0.31 (10)	3.7 (14)	0.2	3.7±0.5	0.50±0.07
	61.2±1.0	0.19	179	324	0.062 (25)	0.63 (26)	<0.1	0.63±0.16	0.08±0.02
	63.0±1.0	0.19	179	324	0.069 (20)	0.73 (21)	<0.1	0.73±0.15	0.09±0.02
	70.1±1.2	0.20	179	324	0.45 (10)	8.1 (18)	0.3	8.1±1.5	1.0±0.2
	78.2±1.3	0.21	179	324	0.21 (15)	3.1 (16)	<0.1	3.1±0.5	0.35±0.06
	80.7±1.4	0.22	179	324	0.12 (20)	1.7 (22)	<0.1	1.7±0.4	0.19±0.04
	84.3±1.5	0.22	179	324	0.32 (15)	5.7 (21)	<0.1	5.7±1.2	0.62±0.13
	86.7±1.6	0.22	179	324	0.23 (15)	3.9 (19)	<0.1	3.9±0.7	0.42±0.08
	93.6±1.8	0.23	179	324	0.85 (10)	32 (26)	0.3	32±8	3.3±0.8
	103±2	0.24	179	324	1.58 (10)	99 (15)	0.4	99±15	9.8±1.4
	106±2	0.25	179	324	0.20 (25)	3.8 (30)	<0.1	3.8±1.1	0.37±0.11
	110±2	0.25	179	324	0.47 (15)	12 (24)	0.2	12±3	1.1±0.3
Hf^{180}	73.9±1.2	0.20	180	204	1.72 (10)	44 (19)	0.7	50±6	5.8±0.7
			Normal	298	1.50 (15)	46 (23)	0.9		
			179	590	1.29 (10)	58 (18)	0.7		

A casual inspection of the relationship of the neutron width to the spacing to the neighboring levels reveals no obvious correlation in the sense that strong levels correspond to large spacing of neighboring levels. The failure of this effect to appear implies that the simple derivation of the proportionality of Γ_n to D usually given[4] is not to be taken too literally, for it would lead one to expect a tendency for the size of Γ_n to be associated with the D in the immediate vicinity.

B. Level Spacing

For the neutron energies used in the present work the neutron resonances observed in a particular nuclide are limited to the two possible J values, $I\pm\frac{1}{2}$, that can be excited by $l=0$ neutrons. In some ways unfortunate, this limitation nevertheless aids in interpretation of the data because the spins of the levels excited, which would be difficult to measure, are known approximately.

The level spacing observed for a given isotope is determined by the spacing for the two sets of levels, with the contribution of each set somewhat uncertain because of lack of knowledge of their relative frequency. The general procedure in the present work has been to assume that $J=I+\frac{1}{2}$ and $J=I-\frac{1}{2}$ levels are equally probable and to determine the spacing for levels of a single J from the data simply by counting the levels in a given energy interval and multiplying by two. The symbol D without a subscript refers to this spacing for a single spin state. Although in principle D can easily be determined by counting the levels in a given energy interval, it is extremely important to determine if levels are being missed because of experimental conditions.

TABLE XI. Neutron widths of resonances of tantalum ($_{73}Ta^{181}$) based on a Γ_γ of 50±10 mv.

E_0 (ev)	Δ (ev)	$(1/n)\times10^{24}$ (cm²/atom)	Area (% error) (ev)	Γ_n (% error) (mv)	r	Weighted Γ_n (mv)	Reduced width Γ_n^0 (mv)
10.38±0.10	0.077	6050	0.118 (8)	4.6 (13)	0.2	4.5±0.5	1.40±0.17
		338	0.58 (7)	4.3 (24)	1.1		
13.95±0.12	0.090	1017	0.113 (10)	0.96 (9)	<0.1	1.04±0.08	0.28±0.02
		338	0.285 (8)	1.35 (16)	0.3		
		38.5	0.69 (10)	1.01 (28)	0.8		
20.5±0.2	0.11	1017	0.088 (12)	1.03 (13)	<0.1	1.12±0.10	0.25±0.02
		338	0.255 (10)	1.33 (16)	0.3		
		38.5	0.61 (6)	0.96 (22)	1.1		
		38.5	0.62 (10)	1.02 (28)	0.7		
22.8±0.3	0.12	338	0.107 (25)	0.48 (33)	<0.1	0.25±0.04	0.052±0.008
		38.5	0.29 (11)	0.20 (18)	0.3		
		38.5	0.30 (20)	0.22 (33)	0.2		
24.0±0.3	0.12	6050	0.092 (25)	7.5 (28)	<0.1	6.1±0.7	1.25±0.15
		1017	0.32 (10)	6.4 (18)	0.3		
		338	0.48 (12)	5.0 (27)	0.3		
		38.5	1.19 (10)	5.8 (25)	0.7		
		38.5	1.14 (15)	5.3 (31)	0.6		
30.1±0.3	0.13	38.5	0.27 (12)	0.23 (21)	0.1	0.23±0.05	0.042±0.009
35.4±0.4	0.14	6050	0.126 (15)	15 (22)	<0.1	17±2	2.9±0.4
		6050	0.156 (20)	20 (27)	<0.1		
		1017	0.49 (15)	18 (25)	0.2		
		338	0.76 (15)	17 (33)	0.3		
36.1±0.4	0.14	6050	0.135 (15)	17 (18)	0.1	18±2	3.0±0.4
		6050	0.156 (20)	21 (23)	0.1		
		1017	0.49 (15)	18 (28)	0.3		
		338	0.76 (15)	17 (32)	0.3		
39.3±0.5	0.15	6050	0.33 (15)	55 (19)	0.1	51±5	8.1±0.8
		6050	0.37 (20)	65 (21)	0.1		
		1017	0.82 (10)	48 (17)	0.3		
		338	1.25 (10)	43 (18)	0.3		
49.4±0.6	0.17	338	0.117 (20)	1.08 (27)	<0.1	1.1±0.3	0.16±0.04
57.5±0.7	0.18	38.5	0.52 (25)	0.5 (48)	0.3	0.5±0.2	0.07±0.03
62.9±0.8	0.19	338	0.39 (15)	8.6 (27)	0.1	10±2	1.25±0.25
		38.5	1.14 (15)	12 (34)	0.5		
77.2±1.3	0.21	338	0.77 (15)	27 (28)	0.2	40±7	4.6±0.8
		38.5	2.63 (10)	47 (19)	0.2		
83.4±1.4	0.22	338	0.69 (15)	21 (29)	0.2	21±6	2.3±0.7
91.3±1.8	0.23	338	0.33 (25)	7 (36)	<0.1	7±2	0.7±0.2
99.8±1.9	0.24	338	1.79 (10)	125 (21)	0.1	125±25	12.5±2.5
106±2	0.25	338	0.56 (20)	16 (38)	<0.1	16±6	1.6±0.6
116±2	0.26	338	1.14 (15)	64 (25)	0.2	64±16	6.0±1.5
127±3	0.27	338	0.70 (20)	28 (36)	<0.1	28±10	2.5±0.9

The analysis of Tm in Sec. III illustrates the method used to establish that all levels in a particular region have been found. In that case, for instance, investigation shows that a level with a Γ_n^0 only $\frac{1}{5}$ of the smallest Γ_n^0 actually obtained could have been identified if present. The absence of levels of this magnitude indicates that levels are not being missed simply because of their small size.

Levels will also be missed, of course, if they merge and are misinterpreted as single levels; this possibility was checked in the case of Tm by observing the rate of appearance of levels with neutron energy. This behavior, Fig. 3, indicates that levels are not missed in Tm until an energy of about 75 ev is reached. Still another way of considering the possibility of missed levels is by means of the size distribution of Γ_n^0, for one can extrapolate the distribution of Fig. 4 back to zero width to obtain the total number of levels in a given energy range, hence the spacing. As this extrapolation covers such a small range in neutron width, it cannot change the total number of levels greatly.

The level spacings thus obtained refer to an excitation energy just above the neutron binding energy, which energy is in the range 5 to 8 Mev for the nuclides considered. Because of the rapid change of D with excitation energy, it is useful to convert the observed spacings to a specific value of the excitation energy for comparison purposes. If very accurate spacings could be obtained for many isotopes by the present method, it might be possible, by comparing spacings for different isotopes, to

TABLE XII. Neutron widths of resonances of uranium ($_{92}U^{238}$) based on a Γ_γ of 25±5 mv for all resonances but the 6.7-ev resonance for which Γ_γ=24±2 mv.

E_0 (ev)	Δ (ev)	$(1/n)\times10^{24}$ (cm²/atom)	Area (% error) (ev)	Γ_n (% error) (mv)	r	Weighted Γ_n (mv)	Reduced width Γ_n^0 (mv)
6.70±0.06	0.054	22 500	0.039 (7)	1.59 (11)	<0.1	1.52±0.07	0.59±0.03
		7460	0.093 (5)	1.51 (8)	0.1		
		284	0.44 (2)	1.47 (9)	2.0		
		141	0.61 (2)	1.53 (9)	2.0		
20.9±0.2	0.096	7460	0.164 (6)	8.6 (7)	0.1	8.5±0.4	1.86±0.11
		7190	0.165 (7)	8.4 (10)	0.2		
		284	0.710 (3)	8.6 (12)	1.4		
37.0±0.3	0.13	14 970	0.193 (7)	33.7 (9)	0.1	32.5±1.9	5.3±0.3
		7190	0.32 (9)	32.5 (16)	<0.1		
		3230	0.46 (5)	31.0 (13)	0.4		
		284	1.30 (3)	32.7 (12)	1.1		
66.5±0.7	0.17	3230	0.34 (8)	26 (12)	0.2	25±2	3.1±0.3
		428	0.76 (12)	21 (31)	0.2		
		85.1	1.41 (7)	23 (20)	0.5		
		33.3	2.2 (15)	25 (33)	0.3		
81.6±0.9	0.19	428	0.18 (32)	1.8 (44)	<0.1	2.1±0.7	0.23±0.08
		33.3	0.77 (18)	2.4 (48)	<0.1		
90±2	0.20	11.1	0.25 (30)	0.08 (40)	<0.1	0.09±0.03	0.009±0.003
		11.1	0.31 (30)	0.11 (45)	<0.1		
104±2	0.21	3230	0.59 (15)	81 (27)	<0.1	65±9	6.4±0.9
		428	1.20 (5)	62 (17)	0.2		
		33.3	3.4 (18)	56 (33)	0.2		
118±2	0.23	428	0.54 (9)	12 (18)	<0.1	15±2	1.4±0.2
		33.3	1.84 (16)	26 (32)	0.3		
146±3	0.27	33.3	0.58 (35)	0.9 (43)	0.1	0.9±0.4	0.07±0.03
166±3	0.27	33.3	1.0 (30)	2.4 (46)	0.2	2.4±1.2	0.19±0.09
192±4	0.29	428	1.64 (8)	127 (20)	0.1	130±20	9.4±1.7
		33.3	5.7 (20)	150 (36)	<0.1		
212±5	0.30	22.2	3.0 (30)	57 (50)	0.1	60±30	4±2
242±6	0.32	22.2	3.0 (25)	60 (43)	0.1	60±30	4±2
258±6	0.33	22.2	0.72 (40)	1.3 (48)	0.1	1.3±0.6	0.08±0.04
278±7	0.35	22.2	2.3 (30)	40 (53)	0.1	40±20	2.4±1.3
297±8	0.36	22.2	2.2 (30)	40 (58)	<0.1	40±20	2.3±1.3
368±9	0.40	22.2	4.5 (25)	130 (42)	<0.1	130±50	7±3
418±10	0.42	22.2	3.0 (35)	80 (60)	<0.1	80±50	4±2

get information on the variation of spacing with excitation energy. However, because of the fact that the results at the present time are limited in number and statistical accuracy, the most profitable procedure seems to be to convert the spacings to a single excitation energy, using the usual empirical formula[4] for level density,

$$w=10^6/D=a\exp(b\sqrt{E^*}). \tag{7}$$

Here w is the number of levels per Mev, E^* is the excitation energy, and a and b are parameters that vary slowly with atomic weight. The level spacings obtained from counting the levels in given energy regions are shown in Table XIII together with the excitation energies to which they correspond, the latter being obtained from neutron binding energies. The spacings converted to 6 Mev by means of Eq. (7) are also given in Table XIII; in most cases the energy correction is not large relative to the variation in D observed. It can be seen from the values of Table XIII and from Fig. 8, where the adjusted D's are given, that the level spacings at a given excitation energy are not a smooth function of atomic weight as would be expected[28] from the statistical model of the nucleus. Instead, a discontinuity of the order of 100 occurs at the 82 neutron shell. Recent unpublished results obtained with the Van de Graaff at Duke University and with fast choppers at Brookhaven and Argonne give a more pronounced discontinuity at 82 neutrons as well as one of about 10^3 at 126 neutrons.

Discontinuities in level spacing near ground at magic numbers is well known and the present results show definitely that the shell structure exerts a large effect on level spacings at 6-Mev excitation as well. The shell effect at high excitation had already been observed in the work of Hughes, Garth, and Levin[29] at excitation energy 1 Mev higher. In their work the level spacings were obtained from the absorption cross section in the

[28] J. M. B. Lang and K. J. Le Couter, Proc. Phys. Soc. (London) **A67**, 586 (1954).

[29] Hughes, Garth, and Levin, Phys. Rev. **91**, 1423 (1953).

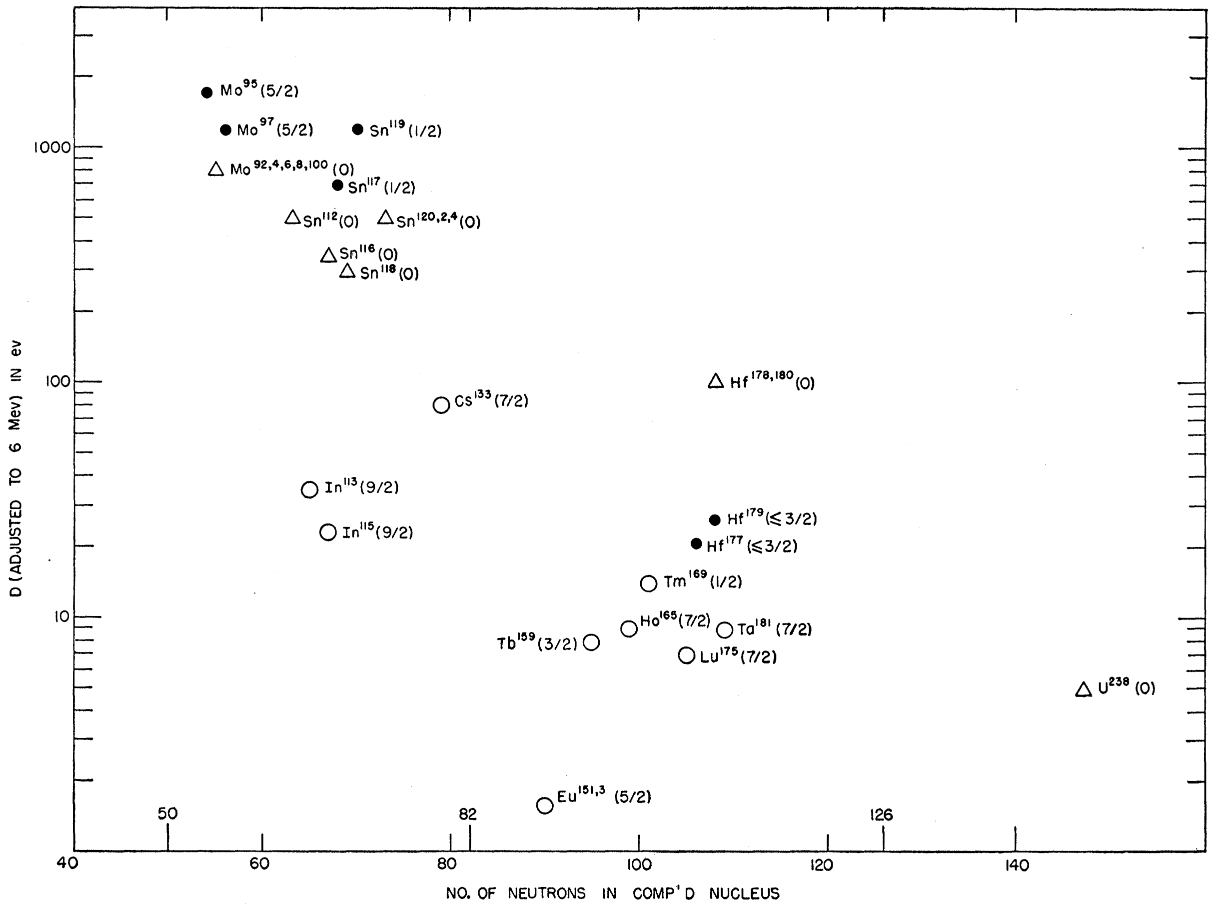

FIG. 8. The level spacings, D, adjusted to 6 Mev, as a function of neutron number in the compound nucleus. Each target nucleus is indicated and its spin is given in parentheses. The symbols ○, ●, and △ refer to odd Z-even N, even Z-odd N, and even Z-even N target nuclei, respectively. Points labeled with several isotopic numbers are averages for the isotopes.

Mev region but required knowledge of Γ_γ in the calculation. The recent measured Γ_γ's show that the assumed values of Γ_γ used by Hughes, Garth, and Levin were approximately correct; however, there is still some uncertainty in their D's because of the unknown contribution of higher l's in their measurements.

It would be very interesting to establish other level-density variations but unfortunately sufficiently many nuclei have not been investigated to establish definite trends. Although some even-odd effects seem to be present in Fig. 8, the data are not extensive enough to establish them definitely. However, one effect that seems definite is the higher D for even-Z nuclei. It would be of great interest to investigate the dependence of D on level spin J; the present data, while not extensive, do not seem to show an effect as large as the $1/(2J+1)$ factor expected theoretically.[28]

C. $\bar{\Gamma}_n^0/D$ Ratio

In addition to the intrinsic interest of $\bar{\Gamma}_n^0$ and D individually, their ratio has an important bearing at present on nuclear models. The significance of the $\bar{\Gamma}_n^0/D$ ratio follows directly from the discussion already given in IV A concerning the composition of neutron widths in terms of the intrinsic lifetime of a nuclear state and the penetrability of the nuclear surface. As the intrinsic lifetime of a state, t_0, is approximately given by h/D, it follows that division of the neutron width by D removes the specific nuclear part, leaving only the penetrability of the nuclear surface,

$$\Gamma_n/D = p/2\pi.$$

The relationship $t_0 = h/D$ follows directly[30] if the levels are considered to have equal spacing and it can be taken to hold approximately for actual level spacings as well, with D the average spacing.

For a strongly absorbing or "black" nucleus, the penetrability of the sharp potential discontinuity that represents the nuclear surface is simply the ratio of the neutron wave vector outside (k) to that inside (K) the nucleus,

$$p = 4k/K = 4(E/V)^{\frac{1}{2}},$$

[30] V. F. Weisskopf, Helv. Phys. Acta 23, 187 (1950).

TABLE XIII. Observed level spacings in ev, corresponding to an excitation energy equal to the neutron binding energy, and the spacings adjusted to 6 Mev as explained in the text.

Target isotope	Spin, I	D (ev)	Excitation energy (Mev)	D (adjusted to 6 Mev) (ev)
${}_{42}Mo^{95}$	5/2	370±120	9.15	1700
${}_{42}Mo^{97}$	5/2	370±120	8.29	1200
${}_{42}Mo^{92, 4, 6, 8, 100}$	0	500±150	6.9	800
${}_{49}In^{113}$	9/2	14±2	7.2	35
${}_{49}In^{115}$	9/2	14±2	6.6	23
${}_{50}Sn^{112}$	0	150±80	8.0	500
${}_{50}Sn^{116}$	0	150±70	7.3	350
${}_{50}Sn^{117}$	1/2	120±30	9.3	700
${}_{50}Sn^{118}$	0	200±100	6.6	300
${}_{50}Sn^{119}$	1/2	300±140	8.6	1200
${}_{50}Sn^{120, 2, 4}$	0	500±200	6.1	500
${}_{55}Cs^{133}$	7/2	42±5	6.73	80
${}_{63}Eu^{151, 3}$	5/2	2.2±0.3	5.7	1.6
${}_{65}Tb^{159}$	3/2	10.0±1.0	5.8	8
${}_{67}Ho^{165}$	7/2	12.0±1.3	5.7	9
${}_{69}Tm^{169}$	1/2	15±2	5.9	14
${}_{71}Lu^{175}$	7/2	7±2	6.0	7
${}_{72}Hf^{177}$	≤3/2	5.6±0.6	7.6	21
${}_{72}Hf^{179}$	≤3/2	8±2	7.4	26
${}_{72}Hf^{178, 180}$	0	100±50	6.1	100
${}_{73}Ta^{181}$	7/2	9.0±1.0	6.03	9
${}_{92}U^{238}$	0	18±2	4.87	5

where E is the neutron energy and V the well depth. Thus the ratio of the average reduced neutron width to the spacing D turns out to be a function of the well depth alone,

$$\frac{\bar{\Gamma}_n^0}{D}=\frac{\langle\Gamma_n/E^{\frac{1}{2}}\rangle_{\text{Av}}}{D}=\frac{4}{2\pi}\left(\frac{1}{V}\right)^{\frac{1}{2}},$$

a ratio that is 1.0×10^{-4} for a 42-Mev well depth, for example.

For a partially transparent nucleus, represented by a potential with a small complex component, the $\bar{\Gamma}_n^0/D$ ratio is not constant with atomic weight but exhibits optical interference maxima. The cloudy crystal ball model gives a ratio with peaks at $A=57$ and 156, these positions being determined by the nuclear radius, R, possessing a simple relationship to the neutron wave number inside the nucleus (K),

$$KR=n\pi+\tfrac{1}{2}\pi,$$

with $n=2$ and 3 for the peaks quoted. The heights of the peaks in the $\bar{\Gamma}_n^0/D$ ratio are fixed by the complex component of the potential; hence it is desirable to check the magnitude and location of the peaks in an investigation of the validity of the model.

Results on the $\bar{\Gamma}_n^0/D$ ratio, based mainly on Brookhaven fast-chopper work, have been published recently.[9] The present data are given in Fig. 9, which is essentially the same as the published results,[9] with a few additional points as well as minor changes in the older results. The curve for a potential well $V=42(1+i0.03)$ Mev, corresponding to the model of Feshbach, Porter, and Weisskopf, is shown for comparison. The experimental results show a peak near the expected atomic weight but of much smaller magnitude and greater width than computed for this particular model. It should be remembered that the parameters of the potential were adjusted to fit the neutron cross sections in the Mev region and not adjusted to fit the $\bar{\Gamma}_n^0/D$ ratio.

The disagreement of the present experimental results with the theoretical curve is probably related to the fact that the Mev cross sections, used to obtain the parameters, are a measure of the potential scattering alone (gross elastic scattering in the terminology of Feshbach *et al.*). The $\bar{\Gamma}_n^0/D$ ratio on the other hand is related to the cross section for formation of the compound nucleus

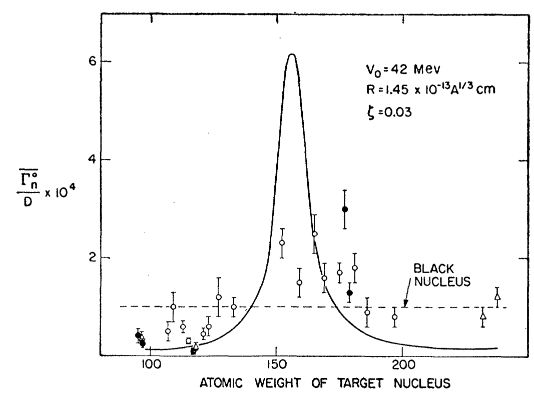

FIG. 9. Comparison of experimental values of $\bar{\Gamma}_n^0/D$ with theoretical predictions of the "black" and the "cloudy crystal ball" models of the nucleus. The symbols ○, ●, and △ refer to odd Z-even N, even Z-odd N, and even Z-even N target nuclei, respectively.

and in the present work is completely separated from the potential scattering. In the resonance energy region it is of course possible to obtain separately the cross section for compound nucleus formation, as is done here, and to get the potential scattering as well. The latter can be accomplished by means of a study of the cross section between resonances although very little has been done on this problem.

On the theoretical side there are several possibilities for modifications of the model that will reduce the compound nucleus formation cross section, and hence lower the $\bar{\Gamma}_n^0/D$ ratio, without changing the potential scattering, which already agrees with the Mev results. These possibilities include changing the sharp nuclear boundary to a diffuse boundary,[31] coupling of the incoming neutron to the low-lying rotational levels,[32]

[31] C. E. Porter and V. F. Weisskopf (private communication).
[32] A. Bohr and B. R. Mottleson (private communication).

and concentrating the cloudiness of the crystal at the nuclear surface.[33] Some of these theoretical possibilities can be tested by means of the $\bar{\Gamma}_n^0/D$ ratio but it would be necessary to increase the number of nuclides studied as well as the statistical accuracy for individual nuclides.

[33] H. Amster and V. F. Weisskopf (private communication).

V. ACKNOWLEDGMENTS

During the course of these measurements, the assistance of R. C. Garth, H. R. Muether, and A. Stolovy in taking data was of great value, as were discussions of theoretical implications with C. E. Porter, V. F. Weisskopf, A. Bohr, and B. R. Mottelson.

PHYSICAL REVIEW VOLUME 99, NUMBER 1 JULY 1, 1955

Photoprotons from Oxygen†

B. M. SPICER*
Physics Research Laboratory, University of Illinois, Champaign, Illinois
(Received January 6, 1955)

The cross section and angular distribution of the $O^{16}(\gamma,p)N^{15}$ reaction have been obtained for photon energies between 13.5 and 18.7 Mev, i.e., below the expected position of the giant resonance. The angular distribution indicated that the reaction proceeded predominantly through electric quadrupole or magnetic dipole absorption of photons, even though electric dipole transitions are allowed by isotopic spin selection rules. Suggestions are made regarding this forbiddenness of electric dipole absorption.

INTRODUCTION

STUDIES of photon absorption in oxygen have almost always used the (γ,α),[1] $(\gamma,4\alpha)$,[2] or (γ,n)[3,4] reactions. The only exception is the work of Wäffler and Younis,[1] who also obtained the (γ,p) cross section at 17.6 Mev, using γ rays from the $Li^7(p,\gamma)Be^8$ reaction.

It has been shown that if the assumption of the charge independence of nuclear forces is made, then it is expected that the (γ,α) reaction is forbidden to proceed via electric dipole absorption for energies below about 25 Mev.[5] This appears to be substantiated by experiment. The work of Penfold and the author[4] on the fine structure in the (γ,n) activation curve suggests that the (γ,n) reaction below 19 Mev proceeds by electric quadrupole and magnetic dipole absorption of photons. However, this suggestion was made on the basis of comparison of radiative widths to relatively inaccurate theoretical estimates. Therefore, it was deemed worthwhile to seek further information on the mechanism of photon absorption in oxygen below 20 Mev.

The experiment reported here was performed to obtain the cross-section and angular distribution for the $O^{16}(\gamma,p)N^{15}$ reaction between 13.5 and 18.7 Mev.

† Supported in part by the joint program of the Office of Naval Research and the U. S. Atomic Energy Commission.

* Fulbright Fellow, on leave from the Physics Department, University of Melbourne, Melbourne, Australia.

[1] H. Wäffler and S. Younis, Helv. Phys. Acta **22**, 614 (1949); Nabholz, Stoll, and Waffler, Phys. Rev. **86**, 1043 (1952).

[2] F. K. Goward and J. J. Wilkins, Proc. Phys. Soc. (London) **A65**, 671 (1952); C. A. Hsaio and V. L. Telegdi, Phys. Rev. **90**, 494 (1953); D. L. Livesey and C. L. Smith, Proc. Phys. Soc. (London) **A65**, 758 (1952).

[3] Katz, Haslam, Horsley, Cameron, and Montalbetti, Phys. Rev. **95**, 464 (1954).

[4] A. S. Penfold and B. M. Spicer (to be published).

[5] M. Gell-Mann and V. L. Telegdi, Phys. Rev. **91**, 169 (1953).

EXPERIMENTAL ARRANGEMENT

The photon source used in this experiment was a bremsstrahlung spectrum of maximum energy 18.7 Mev. The x-ray beam was collimated with lead to a pencil of angular diameter 0.012 radian, or a diameter of 1 cm at the center of the gas target, 90 cm from the source of x-rays. The scattering chamber used was similar to the one described by Fuller.[6] The line-up of the x-ray beam with respect to the scattering chamber was checked before each run by means of pictures of the beam taken on dental x-ray film. These films were positioned accurately with respect to the scattering chamber.

The scattering chamber contained oxygen gas at a pressure of one atmosphere. The gas acted as the target for the x-rays. Protons were detected in a pair of 1×3-inch 100-micron Ilford *G*-Special emulsions, which were placed parallel to, and to one side of, the x-ray beam. The emulsions were 0.87 cm apart, and their near edge was 2.40 cm from the center of the x-ray beam. Two sets of exposures were made, and in each case the dose at the scattering chamber was 5300 roentgens, as indicated by a Victoreen thimble at the center of an 8-cm cube of Lucite.

The emulsions were processed according to the dry development technique described by Beiser.[7] Observations on the tracks were made with two Leitz-Wetzlar binocular microscopes, using ×53 objective and ×8 ocular. This combination gave a field of view that was approximately 200 microns in diameter. Plates were searched by taking six-centimeter swaths along their long dimension.

Measurements made on the proton tracks were the

[6] E. G. Fuller, Phys. Rev. **79**, 303 (1950).

[7] A. Beiser, Revs. Modern Phys. **24**, 273 (1952).